1 CURRENT STATUS OF NEUTRINO MASSES AND OSCILLATIONS

1.1 Neutrino Masses

1.1.1 Laboratory limits

Direct laboratory limits on neutrino masses are obtained from kinematical studies. The most stringent current upper limit is that on the $\bar{\nu}_e$ mass, coming from the Mainz experiment measuring the end-point of the electron energy spectrum in Tritium beta decay [1]

$$m_{\bar{\nu}_e} \leq 2.2 \text{ eV } 95\%\text{CL}$$

The Troitsk group has also published a limit similar to that of the Mainz group of

$$m_{\bar{\nu}_e} \leq 2.1 \text{ eV } 95\%\text{CL}$$

however they must include an ad-hoc step function near the endpoint to avoid the problem of negative mass squared.

The proposed KATRIN experiment aims to improve the sensitivity to $m_{\bar{\nu}_e} \sim 0.3$ eV [3]. Similar sensitivities are the goal of the longer term MARE experiment [4] based on an array of several thousand of microbolometers. These measurements are sensitive to:

$$m_{\bar{\nu}_e} = \left(\sum_i |V_{ei}^2| \; m_i^2 \right)^{1/2} = \left(\cos^2\theta_{13}(m_1^2 \cos^2\theta_{12} + m_2^2 sin^2\theta_{12}) + m_3^2 sin^2\theta_{13} \right)^{1/2} \qquad (1)$$

An important constraint on Majorana neutrino masses arises from neutrinoless double-β decay [7], in which an (A, Z) nucleus decays to $(A, Z + 2) + 2\; e^-$, without any neutrino emission. This process can be used to constrain the combination

$$|m_{\beta\beta}| = \left| \sum_i U_{ei}^{*2} \; m_i \right| = \left| \cos^2\theta_{13}(m_1 \cos^2\theta_{12} + m_2 e^{2i\alpha} sin^2\theta_{12}) + m_3 e^{2i\beta} sin^2\theta_{13} \right|. \qquad (2)$$

which involves a coherent sum over all the different Majorana neutrino masses m_i, weighted by their mixings with the electron flavour eigenstate, which may include CP-violating phases, as discussed below. This observable is therefore distinct from the quantity observed in Tritium β decay.

The interpretation of neutrinoless double-β decay data depends on calculations of the nuclear matrix elements entering in this process.

A claim for a double-β signal has been made by [9] analyzing the Heidelberg-Moscow data on ^{76}Ge:

$$T^{0\nu}_{1/2} = 1.19 \times 10^{25} \text{ years}$$

corresponding to

$$< m_{\beta\beta} >= 0.05 - 0.85 \text{ eV } (95\%\text{CL})$$

the uncertitude coming from the choice of the nuclear matrix element calculation.

This result is in contrast with the limit computed with a combined analysis of the Hedelberg-Moskow and IGEX experiments [10] and to what reported by a separate group of the original collaboration [11], reporting no evidence for a signal.

Recent results on ^{130}Te from the Cuoricino collaboration [12]: $T^{0\nu}_{1/2} > 1.8 \cdot 10^{24}$ years corresponding to $m_{\beta\beta} < .2 - 1.1$ eV and on ^{100}Mo from the NEMO3 collaboration [13]: $T^{0\nu}_{1/2} > 4.6 \cdot 10^{23}$ years corresponding to $m_{\beta\beta} < .7 - 2.8$ eV do not confirm the Germanium claim, but are not sensitive enough to rule out it.

The approved future experiments at LNGS Cuore [14] and Gerda [15] will have the required sensitivity to unambiguously clarify this experimental situation: $m_{\beta\beta} = 0.024 - 0.14$ eV an $m_{\beta\beta} = 0.09 - 0.29$ eV respectively.

1.2 Massive Neutrinos in Cosmology

There are two places in cosmology where the mass of neutrinos would play a significant role. One is leptogenesis in the early universe, and the other is the evolution of mass density fluctuations that are explored with cosmic microwave background (CMB) fluctuations and the formation of cosmic structure. There is one more place where the presence of neutrinos is generally important — primordial nucleosynthesis, but the effect of neutrino mass is negligible unless it is unrealistically heavy.

One of the promising ideas for baryogenesis is the generation of baryon asymmetry via leptogenesis from the Majorana mass term in the presence of the action of sphalerons of electroweak interactions [18]. According to the latest analyses with the Boltzmann equation yield [19, 20, 21], these models work provided that

$$m_{\nu_i} < 0.1\text{eV}, \tag{3}$$

for all species of neutrinos.

This indicated that we are on the right track to understand the cosmic structure formation. In the last ten years all observations converged to pointing towards an universe where dark matter (i.e., dark matter that was non-relativistic when it was decoupled from the thermal bath) dominates the matter component of the Universe, and where the cosmological constant dominates the energy of the Universe. The recent results from WMAP [16] and SDSS [17] strongly supported this standard view based on the ΛCDM Universe, as demonstrated by the convergence of the cosmological parameters [22, 23, 24] to $H_0 = 71 \pm 5\text{km s}^{-1}\text{Mpc}^{-1}$, $\Omega_m = 0.28 \pm 0.03$, $\Omega_\Lambda = 0.72 \pm 0.03$, $\Omega_m + \Omega_\Lambda = 1.01 \pm 0.01$ We also know that baryons amount to only 1/6 of Ω_m, and only 6% of them are comprised in stars and stellar remnants. Another important measure is the power spectrum that characterises matter fluctuations,

$$P(k) = \int d^3x e^{ik\cdot x} \langle \delta(x)\delta(0) \rangle, \tag{4}$$

where $\delta(x)$ is the density contrast at the position x. A variety of observations at vastly different cosmological epochs (CMB at $z = 1090$, galaxy clustering at $z \sim 0.1-0.4$, gravitational lensing at $z \sim 0.5 - 1$, cluster abundances at $z \sim 0.1 - 0.2$), when scaled to $z = 0$, yield $P(k)$ that is described by $|k|^n T(k)$ with $n = 1 \pm 0.02$ and the transfer function $T(k)$ predicted by the ΛCDM model with the cosmological parameters specified above [25, 26] (see Figure 1, left).

The massive neutrinos contribute to the mass density of the Universe by the amount

$$\Omega_\nu = \frac{\sum m_\nu}{94.1 \text{ eV}} h^{-2}, \tag{5}$$

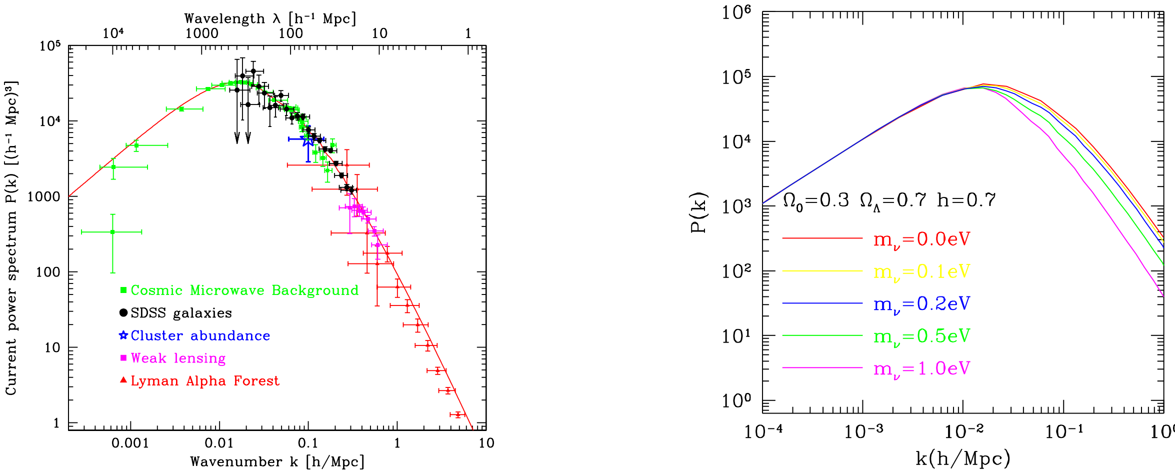

Figure 1: Left: observational power spectrum from CMB fluctuations, galaxy clustering, gravitational lensing shear, cluster abundances and Lyman α clouds, compared with the prediction of ΛCDM model. The figure is taken from the SDSS paper, Tegmark et al. [25]. Right: Power spectrum predicted in the ΛCDM model including massive neutrinos with a degenerate mass specified in the legend. The top curve represents the case of massless neutrinos

where $h = 0.71$ is the conventional notation for the Hubble constant.

A successful model is obtained for cosmic structure formation without having massive neutrinos. This means that massive neutrinos only disturb the agreement between theory and observations, hence leading to a limit on the neutrino mass.

The well-known effect of massive neutrinos is relativistic free streaming that damps fluctuations within the horizon scale. One electron volt neutrinos are still relativistic at matter-radiation equality, which takes place at $T \approx 1$ eV, and then tend to smear fluctuations up to $\sim$100 Mpc comoving scale, thus diminishing the power of $P(k)$ for these scales. This effect becomes stronger as the cosmological mass density of neutrinos, hence the neutrino mass, increases (see Figure 1, right) (see [27, 28]). Therefore, the empirical knowledge of $P(k)$ across large to small scales gives a constraint on the summed mass of neutrinos:
(1) Limits derived from galaxy clustering varies from $\sum m_\nu < 0.6$ eV [22] to 2.1 eV [29] at a 95% confidence, both authors using 2dFGRS data (see also [30]). The limit using the SDSS data is $\sum m_\nu < 1.7$ eV [23]. (See also [31], where $\sum m_\nu < 0.75$ eV is concluded using SDSS and 2dFGRS.)
(2) With the Lyman α cloud absorption power derived from fluctuating optical depths, one can explore $P(k)$ at the smallest scale [32, 33], giving the strongest limit $\sum m_\nu < 0.42$ eV (95%) [34] (see [35] for the earlier work). This result, however, is more model dependent in the sense that one must invoke simulations to extract $P(k)$ from observed flux power spectrum, which suffer from significant uncertainties associated with modelling and simulations.
(3) With gravitational lensing one can directly explore mass fluctuations. For the moment the statistical error is not sufficiently small, but this provides us with a promising method. This may also be used to set the normalisation of the power spectrum derived from galaxy clustering.

Elgarøy and Lahav [36] give a summary of limits obtained in the literature.

1.3 Neutrino Oscillations

The observation of neutrino oscillations has now established beyond doubt that neutrinos have mass and mix. This existence of neutrino masses is in fact the first solid experimental fact requiring physics beyond the Standard Model.

The present status of the field is as follows. Since 1989, we know from LEP [37] that there are only three families of active light neutrinos coupling to the weak interaction.

Since the early 1970's we have hints from solar neutrino experiments that electron neutrinos produced in the sun undergo disappearance on their way to earth, and, from the different disappearance rates for experiments sensitive to different neutrino energy ranges (Chlorine [38], Gallium [39, 40], Water Čerenkov [41]) we have indication that matter effects in the sun play an important role. This "solar neutrino puzzle" was closed in 2002 with the results from the SNO experiment [42], which allowed simultaneously i) a direct measurement of the total flux of active neutrinos by the neutral current reaction in agreement with solar neutrino flux calculations, and ii) a measurement of the electron neutrino component, by the charged current reaction, determining that they represent less than half of the total flux, in agreement with previous observations. The Kamland experiment [43] provided at the same time a measurement of disappearance of electron anti-neutrinos from nuclear fission reactors in Japan, providing, in combination with the solar neutrino results, a precise determination of the relevant neutrino mixing angle of around 300 and of the corresponding mass difference – that can be expressed as an oscillation quarter-wavelength of L/E 15000 km/GeV.

Since the late 80's there has been indication from atmospheric neutrino experiments that the muon neutrinos undergo disappearance when going through the earth; this was finally unambiguously demonstrated by the SuperKamiokaNDE experiment in 1998 [44], a result well supported by Soudan2 [45] and Macro [46] experiments. This disappearance takes place at a much shorter quarter-wavelength than for solar neutrinos (L/E 500km/GeV) [47]; it is not seen for electron neutrinos, a fact that has been best established by the CHOOZ reactor experiment [48]. This disappearance has been confirmed by the K2K experiment in Japan [50], the first accelerator neutrino long baseline experiment designed since neutrino masses have been established, and a prototype for future ones.

The above experimental observations are consistently described by three family ν_1, ν_2, ν_3 with mass values m_1, m_2 and m_3 that are connected to the flavor eigenstates ν_e, ν_μ and ν_τ by a mixing matrix U, usually parameterized as

$$U(\theta_{12},\theta_{23},\theta_{13},\delta_{\rm CP}) = \begin{pmatrix} c_{13}c_{12} & c_{13}s_{12} & s_{13}e^{-i\delta_{\rm CP}} \\ -c_{23}s_{12} - s_{13}s_{23}c_{12}e^{i\delta_{\rm CP}} & c_{23}c_{12} - s_{13}s_{23}s_{12}e^{i\delta_{\rm CP}} & c_{13}s_{23} \\ s_{23}s_{12} - s_{13}c_{23}c_{12}e^{i\delta_{\rm CP}} & -s_{23}c_{12} - s_{13}c_{23}s_{12}e^{i\delta_{\rm CP}} & c_{13}c_{13} \end{pmatrix} \quad (6)$$

where the short-form notation $s_{ij} \equiv \sin\theta_{ij}, c_{ij} \equiv \cos\theta_{ij}$ is used. As a result, the neutrino oscillation probability depends on 3 mixing angles, $\theta_{12}, \theta_{23}, \theta_{13}$, see fig. 2, 2 mass differences, $\Delta m^2_{12} = m^2_2 - m^2_1$, $\Delta m^2_{23} = m^2_3 - m^2_2$, and a CP phase $\delta_{\rm CP}$. Additional phases are present in case neutrinos are Majorana particles, but they do not influence at all neutrino flavor oscillations. Furthermore, the neutrino mass hierarchy, the ordering with which mass eigenstates

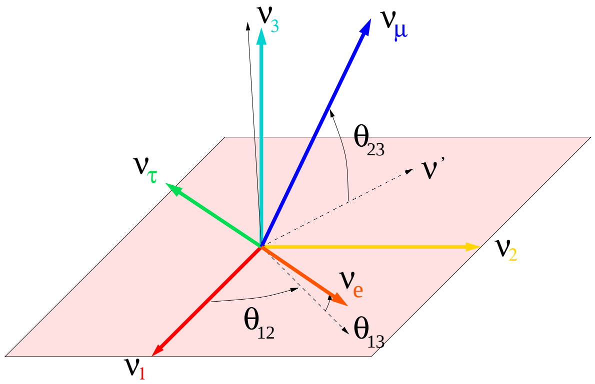

Figure 2: Representation of the 3-dimensional rotation between the flavor and mass neutrino eigenstates

Table 1: Neutrino oscillation parameters as of NUFACT05 [53]

'solar parameters'	$\delta m^2 = \pm(7.92 \pm 0.72) \cdot 10^{-5}$ eV^2	$\sin^2\theta_{12} = 0.314^{+0.030}_{-0.025}$
'atmospheric parameters'	$\Delta m^2 = \pm(2.4^{+0.5}_{-0.6}) \cdot 10^{-3}$ eV^2	$\sin^2\theta_{23} = 0.44^{+0.18}_{-0.10}$
'absolute mass'	$m_\nu \leq 2.2$ eV (tritium decay) $\sum m_\nu = \mathcal{O}(1\text{eV})$ (cosmology)	

are coupled to flavor eigenstates, can be fixed by measuring the sign of Δm^2_{23}. In vacuum the oscillation probability between two neutrino flavors α, β is:

$$P(\nu_\alpha \to \nu_\beta) = -4\sum_{k>j} Re[W^{jk}_{\alpha\beta}]\sin^2\frac{\Delta m^2_{jk}L}{4E_\nu} \pm 2\sum_{k>j} Im[W^{jk}_{\alpha\beta}]\sin^2\frac{\Delta m^2_{jk}L}{2E_\nu} \quad (7)$$

where $\alpha = e, \mu, \tau$, $j = 1, 2, 3$, $W^{jk}_{\alpha\beta} = U_{\alpha j}U^*_{\beta j}U^*_{\alpha k}U_{\beta k}$. In the case of only two neutrino flavor oscillation it can be written as:

$$P(\nu_\alpha \to \nu_\beta) = \sin^2 2\theta \cdot \sin^2\frac{1.27\ \Delta m^2(eV^2)\cdot L(km)}{E_\nu(GeV)}. \quad (8)$$

Therefore two experimental parameters are relevant for neutrino oscillations: the neutrino energy E_ν and the baseline L (distance of the neutrino source from the detector); in the oscillation formula they are combined into the L/E_ν ratio. When neutrinos pass through matter, the oscillation probability is perturbed [51] depending on sign(Δm^2_{23}) [52]. oscillations, with mass eigenstates The fact that solar neutrinos undergo matter effects in the sun allows us to know that $\Delta m^2_{12} \equiv \delta m \equiv m^2_2 - m^2_1 > 0$. Since atmospheric neutrino disappearance has only been observed for muon neutrinos, which couple weakly to electron neutrinos at the relevant wavelength, we cannot (yet) tell the sign of the mass difference Δm^2_{13}, or Δm^2_{23} , or $\Delta m^2 \equiv (\Delta m^2_{13} + \Delta m^2_{23})/2$ as suggested in ref. [53].

The present values of oscillation parameters are summarized in Table 1 and Figure 1.

Before leaving this section on the status of the field, it is worth remembering a further indication of $\overline{\nu}_\mu \to \overline{\nu}_e$ oscillations with a Δm^2 of $0.3 - 20$ eV^2 which comes from the beam dump LSND experiment detecting a 4σ excess of $\overline{\nu}_e$ interactions in a neutrino beam produced by π^+ decays at rest where the $\overline{\nu}_e$ component is highly suppressed ($\sim 7.8{\cdot}10^{-4}$) [54]. The

KARMEN experiment [55], with a very similar technique but with a lower sensitivity (a factor 10 less for the lower Δm^2), and the NOMAD experiment at WANF of CERN SPS [56] (for $\Delta m^2 > 10$ eV^2) do not confirm the result, excluding a large part of the allowed region of the oscillation parameters. The LSND result doesn't fit the overall picture of neutrino oscillations and several non-standard explanations, as for instance sterile neutrinos, have been put forward to solve this experimental conflict. The MiniBooNE experiment at FNAL, presently taking data, is designed to settle this puzzle with a $5\,\sigma$ sensitivity [57]. If it will become true this will lead to even more exciting phenomenology!

1.3.1 Present generation of long-baseline experiments [49]

Over the next five years the present generation of oscillation experiments at accelerators with long-baseline ν_μ beams (Table 2), K2K at KEK [50], MINOS [58] at the NUMI beam from FNAL [59] and ICARUS [60] and OPERA [61] at the CNGS beam from CERN [62] are expected to confirm the atmospheric evidence of oscillations and measure $\sin^2 2\theta_{23}$ and $|\Delta m^2_{23}|$ within $10 \div 15$ % of accuracy if $|\Delta m^2_{23}| > 10^{-3}$ eV^2. K2K and MINOS are looking for neutrino disappearance, by measuring the ν_μ survival probability as a function of neutrino energy while ICARUS and OPERA will search for evidence of ν_τ interactions in a ν_μ beam, the final proof of $\nu_\mu \rightarrow \nu_\tau$ oscillations. K2K has already completed its data taking at the end of 2004, while MINOS has started data taking beginning 2005. CNGS is expected to start operations in the second half of 2006.

Table 2: Main parameters for present long-baseline neutrino beams

Neutrino facility	Proton momentum (GeV/c)	L (km)	E_ν (GeV)	pot/yr (10^{19})
KEK PS	12	250	1.5	2
FNAL NUMI	120	735	3	$20\div 34$
CERN CNGS	400	732	17.4	$4.5\div 7.6$

In all these facilities conventional muon neutrino beams are produced through the decay of π and K mesons generated by a high energy proton beam hitting needle-shaped light targets. Positive (negative) mesons are sign-selected and focused (defocused) by large acceptance magnetic lenses into a long evacuated decay tunnel where ν_μ's ($\overline{\nu}_\mu$'s) are generated. In case of positive charge selection, the ν_μ beam has typically a contamination of $\overline{\nu}_\mu$ at few percent level (from the decay of the residual π^-, K^- and K^0) and $\sim 1\%$ of ν_e and $\overline{\nu}_e$ coming from three-body $K^\pm$, K_0 decays and μ decays. The precision on the evaluation of the intrinsic ν_e to ν_μ contamination is limited by the knowledge of the π and K production in the primary proton beam target. Hadroproduction measurements at 400 and 450 GeV/c performed with the NA20 [63] and SPY [64] experiments at the CERN SPS provided results with $5 \div 7\%$ intrinsic systematic uncertainties.
The CNGS ν_μ beam has been optimized for the $\nu_\mu \rightarrow \nu_\tau$ appearance search. The beam-line design was accomplished on the basis of the previous experience with the WANF beam at CERN SPS [65]. The expected muon neutrino flux at the Gran Sasso site will have an average energy of 17.4 GeV and $\sim 0.6\%$ ν_e contamination for $E_\nu < 40$ GeV. Due to the long-baseline (L=732 Km) the contribution to neutrino beam from the K^0 and mesons produced in the reinteraction processes will be strongly reduced with respect to the WANF [66]: the ν_e/ν_μ ratio is expected to be known within $\sim 3\%$ systematic uncertainty [67].

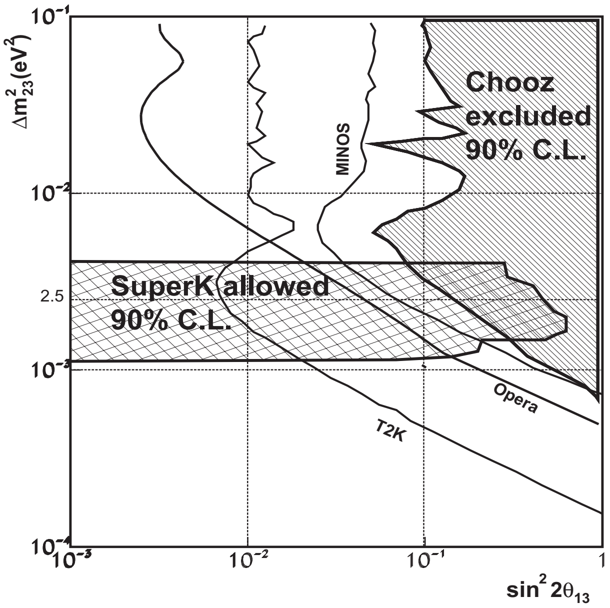

Figure 3: Expected sensitivity on θ_{13} mixing angle (matter effects and CP violation effects not included) for MINOS, OPERA and for the next T2K experiment, compared to the Chooz exclusion plot.

Current long-baseline experiments with conventional neutrino beams can look for $\nu_\mu \to \nu_e$ even if they are not optimized for θ_{13} studies. MINOS at NuMI is expected to reach a sensitivity of $\sin^2 2\theta_{13} = 0.08$ [58] integrating $14{\cdot}10^{20}$ protons on target (pot) in 5 years according to the FNAL proton plan evolution [68]. MINOS main limitation is the poor electron identification efficiency of the detector. OPERA [61] can reach a 90% C.L. sensitivity $\sin^2 2\theta_{13} = 0.060$ ($\Delta m^2_{23} = 2.5{\cdot}10^{-3}$ eV^2, convoluted to CP and matter effects), a factor ~ 2 better than Chooz for five years exposure to the CNGS beam at nominal intensity for shared operation $4.5{\cdot}10^{19}$ pot/yr [69]. Depending on the $\delta_{\rm CP}$ value and matter effects (sign(Δm^2_{23})), these sensitivities can be reduced by a factor ~ 1.5 [70]. According to the CERN PS and SPS upgrade studies [71], the CNGS beam intensity could be improved by a factor 1.5, allowing for more sensitive neutrino oscillation searches for the OPERA experiment.
It is worth mentioning that the sensitivity on θ_{13} measurement of the current long-baseline experiments with conventional neutrino beams, like NUMI and CNGS, will be limited by the power of the proton source which determines the neutrino flux and the event statistics, by the not optimized L/E_ν and by the presence of the ν_e intrinsic beam contamination and its related systematics. This is particular true for CNGS where the neutrino energy, optimized to overcome the kinematic threshold for τ production and to detect the τ decay products, is about ten times higher the optimal value for θ_{13} searches.

Another approach to search for non vanishing θ_{13} is to look at $\overline{\nu}_e$ disappearance using nuclear reactors as neutrino source. A follow-up of Chooz, Double Chooz [72], has been proposed to start in 2008 with a two detectors setup, capable to push systematic errors down to 0.6 % and to reach a sensitivity on $\sin^2 2\theta_{13} \simeq 0.024$ (90% C.L., $\Delta m^2_{23} = 2.5{\cdot}10^{-3}$) in a 3 years run.

A sketch of θ_{13} sensitivities as a function of the time, following the schedule reported in the experimental proposals is reported in Fig. 4

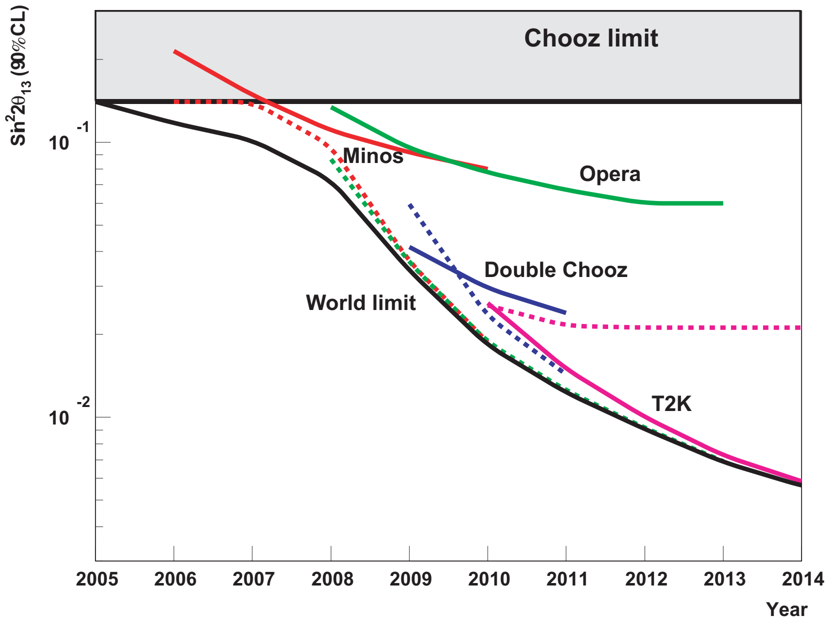

Figure 4: Evolution of sensitivities on $\sin^2 2\theta_{13}$ as function of time. For each experiment are displayed the sensitivity as function of time (solid line) and the world sensitivity computed without the experiment (dashed line). The comparison of the two curves shows the discovery potential of the experiment along its data taking. The world overall sensitivity along the time is also displayed. The comparison of the overall world sensitivity with the world sensitivity computed without a single experiment shows the impact of the results of the single experiment. Experiments are assumed to provide results after the first year of data taking.

1.3.2 Three family oscillations and CP or T violation

It was soon realized that with three families and for a favorable set of parameters, it would be possible to observe violation of CP or T symmetries in neutrino oscillations [73]. This observation reinforced the considerable interest for precision measurements of neutrino oscillation parameters. We know since 2002 and the results from SNO [74] and KAMLAND [43] that the neutrino parameters belong to the so-called LMA solution which suggests that leptonic CP violation should be large enough to be observed in high-energy neutrino oscillation appearance experiments.

This has led to extensive studies, such as those published recently in the CERN yellow report[75], or in a recent BENE [76] workshop on physics at a high intensity proton driver [77]. The phenomenon of CP (ot T) violation in neutrino oscillations manifests itself by a difference in the oscillation probabilities of say, $P(\nu_\mu \rightarrow \nu_e)$vs $P(\overline{\nu}_\mu \rightarrow \overline{\nu}_e)$ (CP violation), or $P(\nu_\mu \rightarrow \nu_e)$vs $p(\nu_e \rightarrow \nu_\mu\ )$ (time reversal violation).

It can be observed right away that observation of this important phenomenon requires appearance experiments; indeed a reactor or solar neutrino experiment, sensitive to the disappearance $P(\nu_e \rightarrow \nu_e)$which is clearly time-reversal invariant, would be completely insensitive to it. This can be seen as an advantage in view of a precise an unambiguous measurement of the mixing angles; for the long term goal of observing and studying CP violation, we are confined to appearance experiments. The $\nu_\mu \rightarrow \nu_e$ transition probability can be parameterized

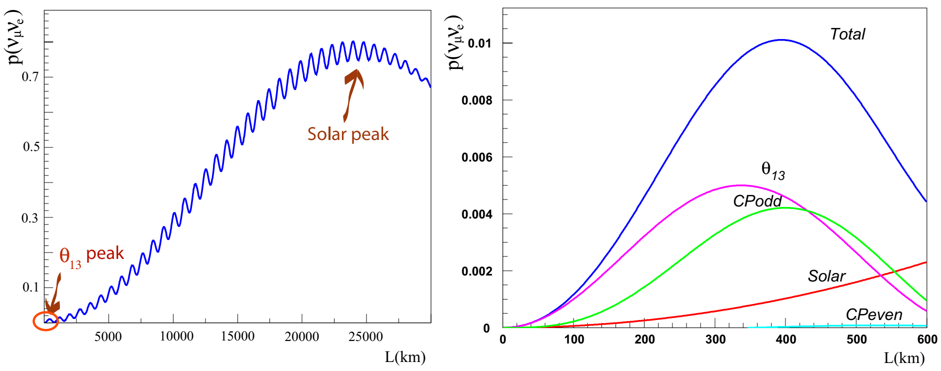

Figure 5: Sketch of $P(\nu_\mu \to \nu_e)$ as function of the baseline computed for monochromatic neutrinos of 1 GeV in the solar baseline regime for $\delta_{\rm CP}$ =0 (left) and in the atmospheric baseline regime for $\delta_{\rm CP} = -\pi/2$ (right), where the different terms of eq. 9 are displayed. The following oscillation parameters were used in both cases: $\sin^2 2\theta_{13} = 0.01$, $\sin^2 2\theta_{12} = 0.8$, $\Delta m^2_{23} = 2.5{\cdot}10^{-3}$ eV^2, $\Delta m^2_{12} = 7{\cdot}10^{-5}$ eV^2. From ref. [49]

as [78]:

$$\begin{aligned}
P(\nu_\mu \to \nu_e) = {} & 4c^2_{13}s^2_{13}s^2_{23}\sin^2\frac{\Delta m^2_{13}L}{4E_\nu} \\
& + 8c^2_{13}s_{12}s_{13}s_{23}(c_{12}c_{23}cos\delta_{\rm CP} - s_{12}s_{13}s_{23})\cos\frac{\Delta m^2_{23}L}{4E_\nu}\sin\frac{\Delta m^2_{13}L}{4E_\nu}\sin\frac{\Delta m^2_{12}L}{4E_\nu} \\
& - 8c^2_{13}c_{12}c_{23}s_{12}s_{13}s_{23}\sin\delta_{\rm CP}\ \sin\frac{\Delta m^2_{23}L}{4E}\sin\frac{\Delta m^2_{13}L}{4E_\nu}\sin\frac{\Delta m^2_{12}L}{4E_\nu} \\
& + 4s^2_{12}c^2_{13}\{c^2_{13}c^2_{23} + s^2_{12}s^2_{23}s^2_{13} - 2c_{12}c_{23}s_{12}s_{23}s_{13}cos\delta_{\rm CP}\}\sin\frac{\Delta m^2_{12}L}{4E_\nu} \\
& - 8c^2_{12}s^2_{13}s^2_{23}\cos\frac{\Delta m^2_{23}L}{4E_\nu}\sin\frac{\Delta m^2_{13}L}{4E_\nu}\frac{aL}{4E_\nu}(1-2s^2_{13}).
\end{aligned} \tag{9}$$

The first line of this parameterization contains the term driven by θ_{13}, the second and third contain CP even and odd terms respectively, and the forth is driven by the solar parameters. The last line parameterizes matter effects developed at the first order where $a[{\rm eV}^2] = \pm 2\sqrt{2}G_F n_e E_\nu = 7.6{\cdot}10^{-5}\rho[g/cm^3]E_\nu[{\rm GeV}]$. The CP odd term and matter effects change sign by changing neutrinos with antinuetrinos.

θ_{13} searches look for experimental evidence of ν_e appearance in excess to what expected from the solar terms. These measurements will be experimentally hard because the Chooz limit on the $\overline{\nu}_e$ disappearance, $\theta_{13} < 11^\circ$ for $\Delta m^2_{23} \simeq 2.5{\cdot}10^{-3}$ eV^2, translates into a $\nu_\mu \to \nu_e$ appearance probability less than 10% at the appearance maximum in a high energy muon neutrino beam.

One of the interesting aspects of this formula is the occurrence of matter effects which, unlike the straightforward θ_{13} term, depends on the sign of the mass difference sign(Δm^2_{23}) . These terms should allow extraction of the mass hierarchy, but could also be seen as a background to the CP violating effect, from which they can be distinguished by the very different

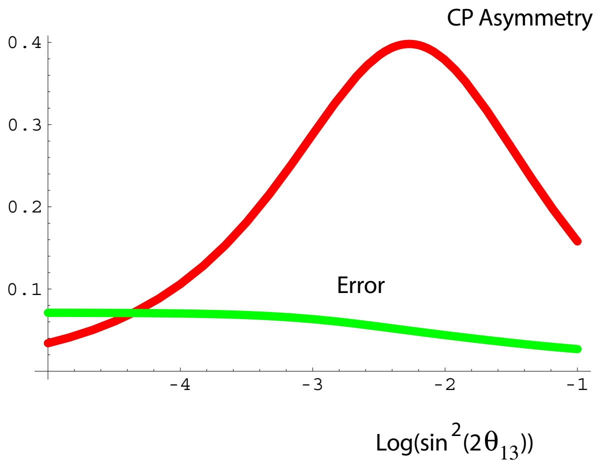

Figure 6: Magnitude of the CP asymmetry at the first oscillation maximum, for $\delta = 1$ as a function of the mixing angle $\sin^2 2\theta_{13}$. The curve marked 'error' indicates the dependence of the statistical+systematic error on such a measurement. The curves have been computed for the baseline Beta Beam option at the fixed energy $E_\nu = 0.4$ GeV, L=130 km, statistical + 2% systematic errors.

neutrino energy dependence, matter effects being larger for higher energies, with a 'matter resonance' at about 12 GeV. The CP violation can be seen as interference between the solar and atmospheric oscillation for the same transition, as emphasized in Figure 3. Of experimental interest is the CP-violating asymmetry A_{CP}:

$$A_{CP} = \frac{P(\nu_\mu \to \nu_e) - P(\overline{\nu}_\mu \to \overline{\nu}_e)}{P(\nu_\mu \to \nu_e) + P(\overline{\nu}_\mu \to \overline{\nu}_e)} \tag{10}$$

displayed in fig. 1.3.2 or the equivalent time reversal asymmetry A_T.

The asymmetry can be large and its value increases for smaller values of θ_{13} up to the value when the two oscillations (solar and atmospheric) are of the same magnitude. The following remarks can be made:

1. The ratio of the asymmetry to the statistical error is fairly independent on θ_{13} for large values of this parameter, which explains the relative flatness of the sensivy curves.

2. This asymmetry is valid for the first maximum. At the second oscillation maximum the curve is shifted to higher values of θ_{13} so that it could be then an interesting possibility for measuring the CP asymmetry, although the reduction in flux is considerable (roughly factor 9).

3. The asymmetry has opposite sign for $\nu_e \to \nu_\mu$ and $\nu_e \to \nu_\tau$, and changes sign when going from one oscillation maximum to the next.

4. The asymmetry is small for large values of θ_{13} placing a challenging emphasis on systematics in the cross-section measurements.

The richness of the $\nu_\mu \to \nu_e$ transition is also its weakness: it will be very difficult for pioneering experiments to extract all the genuine parameters unambiguously. Correlations are present between θ_{13} and $\delta_{\rm CP}$ [79]. Moreover, in absence of information about the sign of Δm^2_{23} [80, 81] and the approximate $[\theta_{23}, \pi/2 - \theta_{23}]$ symmetry for the atmospheric angle [82], additional clone solutions rise up. In general, the measurement of $P(\nu_\mu \rightarrow \nu_e)$ and $P(\bar{\nu}_\mu \rightarrow \bar{\nu}_e)$ will result in eight allowed regions of the parameter space, the so-called eightfold-degeneracy [81].

As already pointed out, the $\nu_\mu \rightarrow \nu_e$ experimental sensitivity with conventional ν_μ beams is limited by an unavoidable ν_e beam contamination of about 1%. The ν_μ to ν_τ oscillations, with E_ν above the τ mass production threshold, generate background due to a significant number of ν_τ charged current interactions where a large fraction of τ's decay into electrons. Finally, neutral pions in both neutral current or charged current interactions can fake an electron providing also a possible background for the ν_e's.
Therefore the measurement of θ_{13} mixing angle and the investigation of the leptonic CP violation will require:

- neutrino beams with high performance in terms of intensity, purity and low associated systematics. Event statistics, background rates and systematic errors will play a decisive role in detecting ν_e appearance;

- the use of detectors of unprecedent mass, granularity and resolution. Again event statistics is the main concern, while high detector performances are necessary to keep the event backgrounds (as π° from ν_μ neutral current interactions, mis-identified as ν_e events) at low as possible rate;

- ancillary experiments to measure the meson production (for the neutrino beam knowledge), the neutrino cross-sections, the particle identification capability. The optimization of proton driver characteristics and the best possible estimation of the systematic errors will require this kind of dedicated experiments. The Harp hadroproduction experiment at CERN PS [83] took data for primary protons between 3 and 14.5 GeV in 2001 and 2002 with different target materials. These data are expected to contribute to the proton driver optimization, the determination of the K2K and MiniBooNE neutrino beam fluxes and to the study of atmospheric neutrino interaction rates.

The intrinsic limitations of conventional neutrino beams are overcome if the neutrino parents can be fully selected, collimated and accelerated to a given energy. This can be attempted within the muon or a beta decaying ion lifetimes. The neutrino beams from their decays would then be pure and perfectly predictable. The first approach brings to the Neutrino Factories [84], the second to the BetaBeams [85]. However, the technical difficulties associated with developing and building these novel conception neutrino beams suggest for the middle term option to improve the conventional beams by new high intensity proton machines, optimizing the beams for the $\nu_\mu \rightarrow \nu_e$ oscillation searches (SuperBeams).
Different detection techniques of neutrino interactions based on water Čerenkov (WC), liquid Argon (LAr), nuclear emulsions and calorimetry are available to build very massive detectors according to the intrinsic neutrino beam characteristics, energy and composition as discussed in the following section.

2 DESCRIPTION OF THE FACILITIES

According to the present experimental situation, conventional neutrino beams can be improved and optimized for the $\nu_\mu \to \nu_e$ searches. The design of a such new SuperBeam facility for a very high intensity and low energy ν_μ flux will demand:

- a new higher power proton driver, exceeding the megawatt, to deliver more intense proton beams on target;
- a tunable L/E_ν in order to explore the Δm^2_{23} parameter region as indicated by the previous experiments with neutrino beams and atmospheric neutrinos;
- narrow band beams with $E_\nu \sim 1 \div 2$ GeV;
- a lower intrinsic ν_e beam contamination which can be obtained suppressing the K^+ and K^0 production by the primary proton beam in the target.

An interesting option for the SuperBeams is the possibility to tilt the beam axis a few degrees with respect to the position of the far detector (Off-Axis beams) [87, 88]. According to the two body π-decay kinematics, all the pions above a given momentum produce neutrinos of similar energy at a given angle $\theta \neq 0$ with respect to the direction of parent pion (contrary to the $\theta = 0$ case where the neutrino energy is proportional to the pion momentum). These neutrino beams have several advantages with respect to the corresponding on-axis ones: they are narrower, lower energy and with a smaller ν_e contamination (since ν_e mainly come from three body decays) although the neutrino flux can be significantly smaller.

2.1 Off axis superbeams: T2K, T2HK and NoνA

The T2K (Tokai to Kamioka) experiment will aim neutrinos from the Tokai site to the Super-KamiokaNDE detector 295 km away. The neutrino beam is produced by pion decay from a horn focused beam, with a system of three horns and reflectors. The decay tunnel length (130 m long) is optimized for the decay of 2-8 GeV pions and short to minimize the occurrence of muon decays. The neutrino beam is situated at an angle of 2-3 degrees from the direction of the Super-Kamiokande detector, assuring a pion decay peak energy of 0.6 GeV. The beam line is equipped with a set of dedicated on-axis and off-axis detectors at two different distances, 280 meters, and possibly, at a later stage, 2 km.

The main goals of the experiment are as follows:

1. The highest priority is the search for ν_e appearance . This reaction is driven by the yet unknown mixing angle θ_{13} , which is also driving the CP violation asymmetry which could be observed in the same channel by comparing neutrino oscillations to antineutrino oscillations. The main challenge here is the understanding of the backgrounds that produce or mimic an electromagnetic shower: beam ν_e from K and muon decay; π° production by neutral current events. It is expected that the sensitivity of the experiment will be of the order of $\sin^2 2\theta_{13} \leq 0.006$.
2. Disappearance measurements of ν_μ. This will improve measurement of Δm^2_{13} down to a precision of a 0.0001 eV^2 or so. The exact measurement of the maximum disappearance is a precise measurement of $\sin^2 2\theta_{23}$. These precision measurements of already known

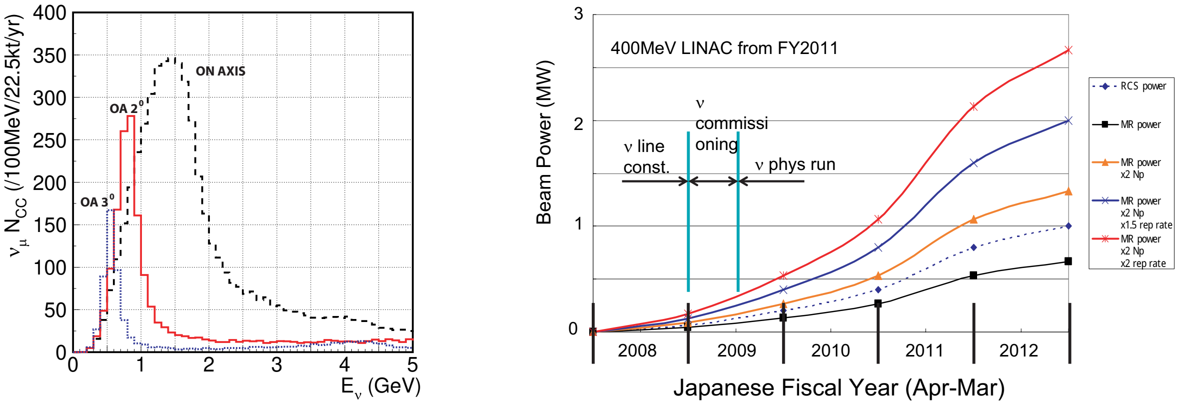

Figure 7: Left: T2K neutrino beam energy spectrum for different off-axis angle θ. Right: expected evolution of T2K beam power as function of time. Baseline option is the second lowest curve.

quantities require good knowledge of flux shape, absolute energy scale, experimental energy resolution and of the cross-section as a function of energy.

3. Neutral current disappearance (in events tagged by π° production) will allow for a sensitive search of sterile neutrino production.

The T2K experiment is planned to start in 2009 with a beam intensity reaching 1 MW beam power on target after a couple years, see fig. 4. It has an upgrade path which involves: a 2km near detector station featuring a water Cherenkov detector, a muon monitor and a fine grain detector (possibly liquid argon); a increase of beam power up to the maximum feasible with the accelerator and target (4 MW beam power?); and a very large water Cherenkov (HyperKamiokande) with a rich physics programme in proton decay, atmospheric and supernova neutrinos and, perhaps, leptonic CP violation, that could be built around in about 15-20 years from now.

The NOνA experiment with an upgraded NuMI Off-Axis neutrino beam [89] ($E_\nu \sim 2$ GeV and a ν_e contamination less than 0.5%) and with a baseline of 810 Km (12 km Off-Axis), was recently proposed at FNAL with the aim to explore the $\nu_\mu \to \nu_e$ oscillations with a sensitivity 10 times better than MINOS. If approved in 2006 the experiment could start data taking in 2011. The NuMI target will receive a 120 GeV/c proton flux with an expected intensity of $6.5 \cdot 10^{20}$ pot/year ($2 \cdot 10^7$ s/year are considered available to NuMI operations while the other beams are normalized to 10^7 s/year). The experiment will use a near and a far detector, both using liquid scintillator. In 5 years of data taking, with 30 Kt active mass far detector a sensitivity on $\sin^2 2\theta_{13}$ slightly better than T2K, as well as a precise measurement of $|\Delta m^2_{23}|$ and $\sin^2 2\theta_{23}$, can be achieved. NOνA can also allow to solve the mass hierarchy problem for a limited range of the $\delta_{\rm CP}$ and sign(Δm^2_{23}) parameters [89].
As a second phase, the new proton driver of 8 GeV/c and 2 MW, could increase the NuMI beam intensity to $17.2 \div 25.2 \cdot 10^{20}$ pot/year, allowing to improve the experimental sensitivity by a factor two and to initiate the experimental search for the CP violation.

2.2 SPL SuperBeam

In the CERN-SPL SuperBeam project [91, 93, 95] the planned 4MW SPL (Superconducting Proton Linac) would deliver a 2.2 GeV/c proton beam, on a Hg target to generate an intense

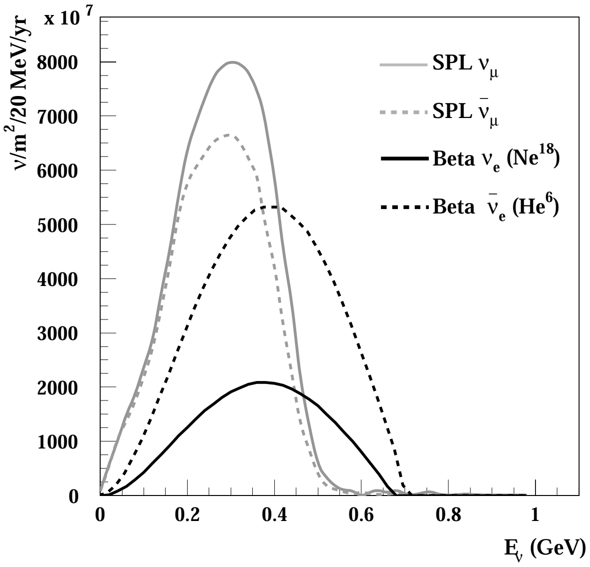

Figure 8: Neutrino flux of β-Beam ($\gamma = 100$) and CERN-SPL SuperBeam, 3.5 GeV, at 130 Km of distance.

π^+ (π^-) beam focused by a suitable magnetic horn in a short decay tunnel. As a result an intense ν_μ beam, will be produced mainly via the π-decay, $\pi^+ \rightarrow \nu_\mu\ \mu^+$ providing a flux $\phi \sim 3.6{\cdot}10^{11}\nu_\mu$/year/m^2 at 130 Km of distance, and an average energy of 0.27 GeV. The ν_e contamination from K will be suppressed by threshold effects and the resulting ν_e/ν_μ ratio ($\sim$ 0.4%) will be known within 2% error. The use of a near and far detector (the latter at $L = 130$ Km of distance in the Frejus area [94]) will allow for both ν_μ-disappearance and $\nu_\mu \rightarrow \nu_e$ appearance studies. The physics potential of the 2.2 GeV SPL SuperBeam (SPL-SB) with a water Cerenkov far detector fiducial mass of 440 Kt [98] has been extensively studied [93].

New developments show that the potential of the SPL-SB potential could be improved by rising the SPL energy to 3.5 GeV [96], to produce more copious secondary mesons and to focus them more efficiently. This seems feasible if status of the art RF cavities would be used in place of the old foreseen LEP cavities [97]. In this upgraded configuration neutrino flux could be increased by a factor 3 with with respect to the 2.2 GeV configuration, reaching a sensitivity to $\sin^2 2\theta_{13}$ 8 times better than T2K and allowing to discovery CP violation (at 3 σ level) if $\delta_{\rm CP} \geq 25^\circ$ and $\theta_{13} \geq 1.4^\circ$ [103]. The expected performances are shown in Fig. 10.

2.3 BetaBeams

BetaBeams (βB) have been introduced by P. Zucchelli in 2001 [85]. The idea is to generate pure, well collimated and intense ν_e ($\overline{\nu}_e$) beams by producing, collecting, accelerating radioactive ions and storing them in a decay ring in 10 ns long bunches, to suppress the atmospheric neutrino backgrounds. The resulting βB would be virtually background free and fluxes could be easily computed by the properties of the beta decay of the parent ion and by its Lorentz boost factor γ. The best ion candidates so far are ^{18}Ne and ^{6}He for ν_e and $\overline{\nu}_e$ respectively. The schematic layout of a Beta Beam is the following (see also fig. 9):

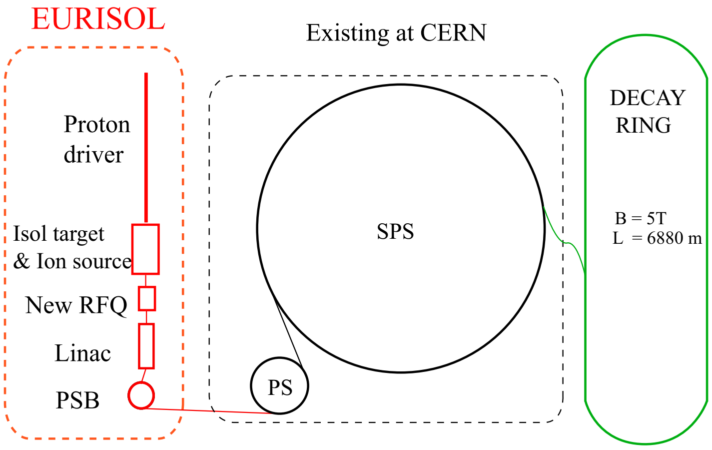

Figure 9: A schematic layout of the BetaBeam complex. At left, the low energy part is largely similar to the EURISOL project [99]. The central part (PS and SPS) uses existing facilities. At right, the decay ring has to be built.

Ion production Protons are delivered by a high power Linac. Beta Beam targets need 100 μA proton beam, at energies between 1 and 2 GeV.

In case the Super Proton Linac (SPL) [91] would be used, Beta Beams could be fired to the same detector together with a neutrino SuperBeam [92]. SPL is designed to deliver 2mA of 2.2 GeV (kinetic energy) protons, in such a configuration Beta Beams would use 10% of the total proton intensity, leaving room to a very intense conventional neutrino beam.

The ^{6}He target consists either of a water cooled tungsten core or of a liquid lead core which works as a proton to neutron converter surrounded by beryllium oxide [100], aiming for 10^{15} fissions per second. ^{18}Ne can be produced by spallation reactions, in this case protons will directly hit a magnesium oxide target. The collection and ionization of the ions is performed using the ECR technique [101].

This stage could be shared with nuclear physicists aiming to a source of radioactive ions of the same intensity to what needed by a Beta Beam. A design study has been recently approved by E.U.: Eurisol [99], where both nuclear and neutrino physics issues will be studied.

Ion acceleration The CERN PS and SPS can be used to accelerate the ions. There is a well established experience at CERN about ion accelerators. Ions are firstly accelerated to MeV/u by a Linac and to 300 MeV/u, in a single batch of 150 ns, by a rapid cycling synchrotron . 16 bunches (consisting of 2.5 10^{12} ions each in the case of ^{6}He) are then accumulated into the PS, and reduced to 8 bunches during their acceleration to intermediate energies. The SPS will finally accelerate the 8 bunches to the desired energy using a new 40 MHz RF system and the existing 200 MHz RF system, before ejecting them in batches of four 10 ns bunches into the decay ring. The SPS could accelerate ^{6}He ions at a maximum γ value of $\gamma_{^6\mathrm{He}} = 150$.

Decay ring The decay ring has a total length of 6880 m and straight sections of 2500 m each (36% useful length for ion decays). These dimensions are fixed by the need to bend ^{6}He ions up to $\gamma = 150$ using 5 T superconducting magnets. Due to the relativistic time dilatation, the ion lifetimes reach several minutes, so that stacking the ions in the decay ring is mandatory to get enough decays and hence high neutrino fluxes. The challenge is then to inject ions in the decay ring and merge them with existing high density bunches. As

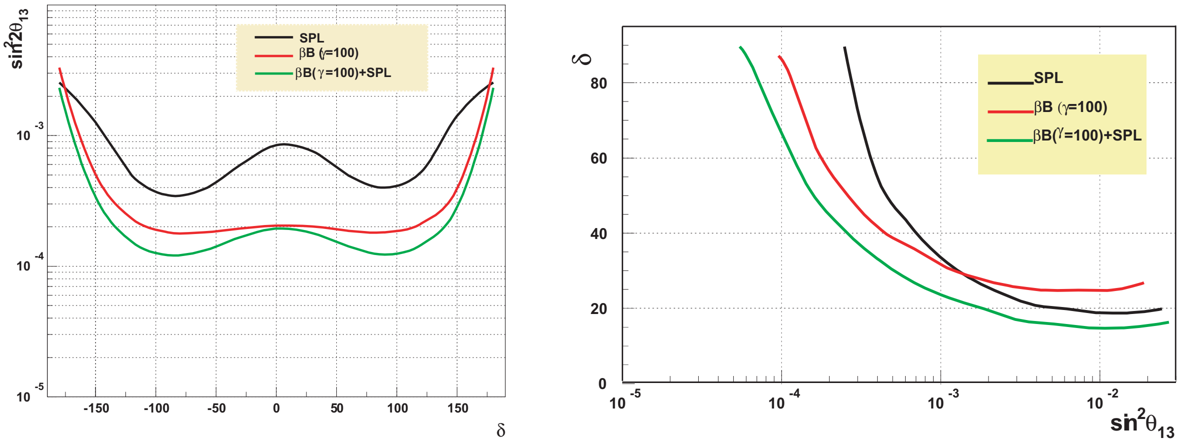

Figure 10: LEFT: θ_{13} 90% C.L. sensitivity as function of $\delta_{\rm CP}$ for $\Delta m^2_{23} = 2.5{\cdot}10^{-3} eV^2$, sign$(\Delta m^2_{23}) = 1$, 2% systematic errors. SPL-SB sensitivities have been computed for a 10 years ν_μ run, βB and βB$_{100,100}$ for a 10 years ν_e+ $\overline{\nu}_e$ run. RIGHT: $\delta_{\rm CP}$ discovery potential at 3σ (see text) computed for 10 years running time. The SPL-SB 3.5 GeV, BetaBeam with $\gamma = 100, 100$ and their combination are shown.

conventional techniques with fast elements are excluded, a new scheme (asymmetric merging) was specifically conceived [102] Summarizing, the main features of a neutrino beam based on the BetaBeams concept are:

- the beam energy depends on the γ factor. The ion accelerator can be tuned to optimize the sensitivity of the experiment;
- the neutrino beam contains a single flavor with an energy spectrum and intensity known a priori. Therefore, unlike conventional neutrino beams, close detectors are not necessary to normalize the fluxes;
- neutrino and anti-neutrino beams can be produced with a comparable flux;
- differently from SuperBeams, BetaBeams experiments search for $\nu_e \rightarrow \nu_\mu$ transitions, requiring a detector capable to identify muons from electrons. Moreover, since the beam does not contain ν_μ or $\bar{\nu}_\mu$ in the initial state, magnetized detectors are not needed. This is in contrast with the neutrino factories (see below) where the determination of the muon sign is mandatory.

A baseline study for a Beta Beam complex (Fig. 9) has been carried out at CERN [105]. The reference βB fluxes are $5.8{\cdot}10^{18}$ ^{6}He useful decays/year and $2.2{\cdot}10^{18}$ ^{18}Ne decays/year if a single ion specie circulates in the decay ring.

The water Čerenkov could be a suitable technology for a large detector. The physics potential has been computed in [106] for $\gamma_{^6{\rm He}} = 60$, $\gamma_{^{18}{\rm Ne}} = 100$ and with a 440 kton detector at 130 km, they are displayed in Fig. 10.

Beta Beam performances have been computed in [106], [107]. The most updated sensitivities for a Beta Beam In this scheme both ions are accelerated at $\gamma = 100$, the optimal setup for the CERN-Frejus baseline of 130 km, have been computed in [104]. The θ_{13} sensitivity curve, computed with a 6 parameters fit minimized over the solar and the atmospheric parameters and projected over θ_{13} , is shown in fig. 10 [104]. Degeneracies induced by the unknown values of sign(Δm^2_{23}) and θ_{23} are not accounted for.

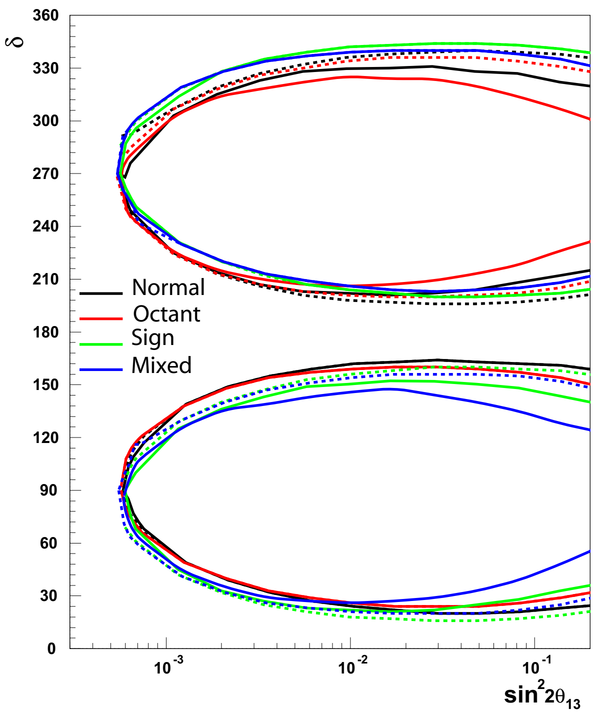

Figure 11: Leptonic CP violation discovery potential at $3\sigma(\Delta\chi^2 > 9.0)$ computed for the 4 different options about the true values of $\mathrm{sign}(\Delta m^2_{23})$ and θ_{23} and including all the possible degeneracies (see text). Dotted curves are computed neglecting the effects of the clone solutions. Taken for ref. [104]

The leptonic CP violation discovery potential at three sigmas ($\Delta\chi^2 = 9.0$), shown in fig. 2.3, has been computed taking into account all the parameter errors and all the possible degeneracies [104]. As common practice in literature $\theta_{23} = 40°$ has been used, to leave room for the octant ($\pi/4 - \theta_{23}$) degeneracy. The discovery potential is computed under 4 different hypotheses of the true parameters, normal: $\mathrm{sign}(\Delta m^2_{23})$ =1, $\theta_{23} < \pi/4$; sign: $\mathrm{sign}(\Delta m^2_{23})$ =-1, $\theta_{23} < \pi/4$; octant: $\mathrm{sign}(\Delta m^2_{23})$ =1, $\theta_{23} > \pi/4$; mixed: $\mathrm{sign}(\Delta m^2_{23})$ =-1, $\theta_{23} > \pi/4$. Each of these 4 true values combinations has been fitted with the 4 possible fit combinations of $\mathrm{sign}(\Delta m^2_{23})$ and θ_{23}. Also shown are the LCPV discovery potentials neglecting the degenerate solutions. Effect of degeneracies are sometimes visible for high values of θ_{13}, precisely the region where they can be reduced by a combined analysis with atmospheric neutrinos [114].

BetaBeams require a proton driver in the energy range of 1-2 GeV, 0.5 MWatt power. The SPL can be used as injector, at most 10% of its protons would be consumed. This allows a simultaneous βB and SPL-SB run, the two neutrino beams having similar neutrino energies. The same detector could then be exposed to 2×2 beams (ν_μ and $\overline{\nu}_\mu \times \nu_e$ and $\overline{\nu}_e$) having access to CP, T and CPT violation searches in the same run. This is particularly important because CP and T channels would have different systematics and different backgrounds, allowing for independent checks of the same signal. Furthermore the SPL ν_μ and $\overline{\nu}_\mu$beams would be the ideal tool to measure signal cross sections in the close detector.

With this combination of neutrino beams a sensitivity to $\sin^2 2\theta_{13}$ 35 times better than T2K could be reached exploiting a CP violation discovery potential at 3 σ if $\delta_{\mathrm{CP}} \geq 18°$ and $\theta_{13} \geq 0.55°$ [103] (Figs. 10).

BetaBeam capabilities for the maximum values of γ available with the SPS, γ^6He = 150

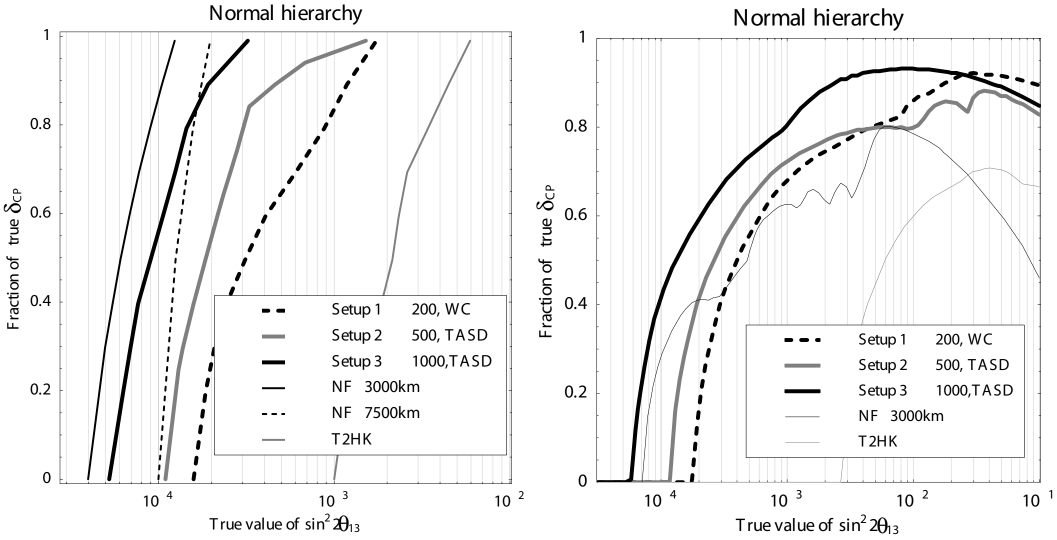

Figure 12: RIGHT: The $\sin^2 2\theta_{13}$ discovery reach (including systematics and correlations) for different setups as function of the true values of $\sin^2 2\theta_{13}$ and $\delta_{\rm CP}$ (3σ confidence level). The values of $\delta_{\rm CP}$ are "stacked" to the fraction of $\delta_{\rm CP}$, i.e., $\sin^2 2\theta_{13}$ will be discovered for a certain fraction of all possible values of $\delta_{\rm CP}$. For a uniform probability contribution in $\delta_{\rm CP}$, the fraction of $\delta_{\rm CP}$ directly corresponds to the probability to discover $\sin^2 2\theta_{13}$. Taken from [115]. LEFT: The sensitivity to CP violation for the normal (left) and inverted (right) mass hierarchy for different experiments as function of the true values of $\sin^2 2\theta_{13}$ and $\delta_{\rm CP}$ at the 3σ confidence level. Taken from [115]

have been computed in [109].

BetaBeam capabilities for ions accelerated at higher energies than those allowed by SPS have been firstly computed in [110] and subsequently in [109, 111, 115]. These studies assume that the same ion fluxes of the baseline scenario can be maintained. However, this is not the case if the number of stored bunches is kept constant in the storage ring. On the other hand, by increasing γ (i.e. the neutrino energy) the atmospheric neutrinos background constraint on the total bunch length [85] tends to vanish. Studies are in progress at CERN in order to define realistic neutrino fluxes as a function of γ [108].

Performances of these higher energy Beta Beams would be anyway extremely interesting, as shown in the plots of fig. 12.

It is worth noting that if a high intensity Beta Beam with $\gamma \sim 300 \div 500$ (requiring a higher energy accelerator than SPS, like the Super-SPS[112]) can be built, a 40 kton iron calorimeter located at the Gran Sasso Laboratory will have the possibility to discover a non vanishing δ_{CP} if $\delta_{\rm CP} > 20^\circ$ for $\theta_{13} \geq 2^\circ$ (99% C.L.) and measure the sign of Δm^2_{23}[116].

A very recent development of the Beta Beam concept is the conceptual possibility to have monochromatic, single flavor neutrino beams thanks to the electron capture process [117, 118]. A suitable ion candidate exists: ^{150}Dy and the performance have been already delineated [117].

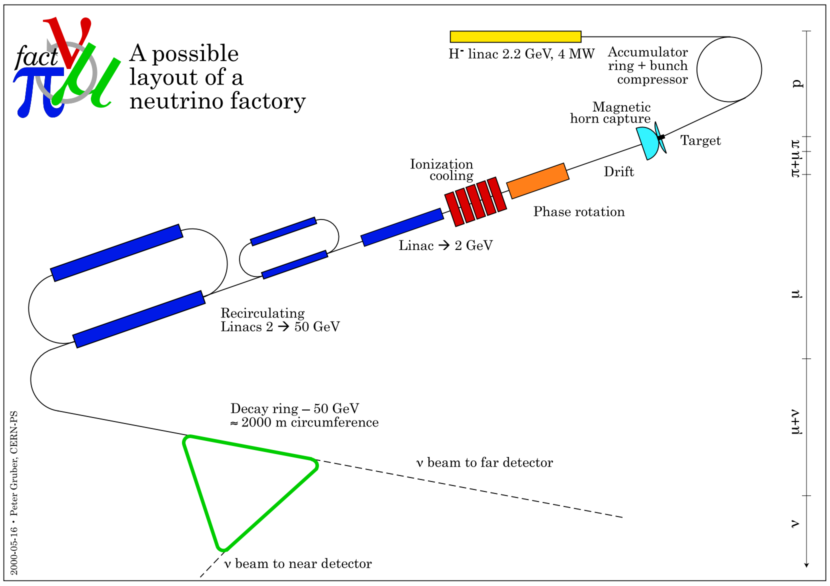

Figure 13: Schematic layout of a Neutrino Factory.

2.4 The Neutrino Factory

In a Neutrino Factory [121] muons are accelerated from an intense source to energies of several GeV, and injected in a storage ring with long straight sections. The muon decays:

$$\mu^+ \to e^+ \nu_e \overline{\nu}_\mu \quad \text{and} \quad \mu^- \to e^- \overline{\nu}_e \nu_\mu$$

provide a very well known flux with energies up to the muon energy itself. The overall layout is shown in Figure 14.

Neutrino Factory designs have been proposed in Europe [122], [123], the US [124] [125][86], and Japan [132]. Of these designs, the american one is the most developed, and we will use it as a example in general with a few exceptions. The conclusions of these studies is that, provided sufficient resources, an accelerator complex capable of providing about 10^{21} muons per year can be built. The Neutrino Factory consists of the following subsystems:

Proton Driver. Provides 1-4 MW of protons on a pion production target. For the Neutrino Factory application the energy of the beam within 4-30 GeV is not critical, since it has been shown that the production of pions is roughly proportional to beam power. The time structure of the proton beam has to be matched with the time spread induced by pion decay (1-2 ns); for a linac driver such as the SPL, this requires an additional accumulator and compressor ring.

Target, Capture and Decay. A high-power target sits within a 20T superconducting solenoid, which captures the pions. The high magnetic field smoothly decreases to 1.75T downstream of the target, matching into a long solenoid decay channel. A design with horn collection has been proposed at CERN for the Neutrino Factory, with the benefit that it can be also used for a superbeam design. The advantage of the horn that it sign-selects the pions and muons is compensated by the fact that in a Neutrino Factory design one could accelerate

Table 3: Comparison of unloaded Neutrino Factory costs estimates in M$ for the US Study II design and improvement estimated for the latest updated US design (20 GeV/c muons). Costs are shown including A: the whole complex; B no Proton Driver and C: no proton driver and no Target station in the estimates. Table from Ref. [128].

Costs in M$	A	B	C
Old estimate from Study II	1832	1641	1538
Multiplicative factor for new estimate	0.67	0.63	0.60

both signs of muons, thus doubling the available flux.

Bunching and Phase Rotation. The muons from the decaying pions are bunched using a system of rf cavities with frequencies that vary along the channel. A second series of rf cavities with higher gradients is used to rotate the beam in longitudinal phase-space, reducing the energy spread of the muons. Cooling. A solenoid focusing channel with high-gradient 201 MHz rf cavities and either liquid-hydrogen or LiH absorbers is used to reduce the transverse phase-space occupied by the beam. The muons lose, by dE/dx losses, both longitudinal- and transverse-momentum as they pass through the absorbers. The longitudinal momentum is replaced by re-acceleration in the rf cavities.

Acceleration. The central momentum of the muons exiting the cooling channel is 220 MeV/c. A superconducting linac with solenoid focusing is used to raise the energy to 1.5 GeV. Thereafter, a Recirculating Linear Accelerator raises the energy to 5 GeV, and a pair of Fixed-Field Alternating Gradient rings accelerate the beam to at least 20 GeV.

Storage Ring. A compact racetrack geometry ring is used, in which 35% of the muons decay in the neutrino beam-forming straight section. If both signs are accelerated, one can inject in two superimposed rings or in two parallel straight sections. This scheme produces over $6 \cdot 10^{20}$ useful muon decays per operational year and per straight in a triangular geometry.

The European Neutrino Factory design is similar to the US design, but differs in the technologies chosen to implement the subsystems.

The Japanese design is quite different, and uses very large acceptance accelerators. Cooling, although it would improve performance, is not considered mandatory in this scheme.

An important Neutrino Factory R&D effort is ongoing in Europe, Japan, and the U.S. since a few years. Significant progress has been made towards optimizing the design, developing and testing the required components, and reducing the cost.

To illustrate this progress, the cost estimate for a recent update of the US design [128] is compared in Table 2 with the corresponding cost for the previous "Study II" US design [86]. It should be noted that the Study II design cost was based on a significant amount of engineering input to ensure design feasibility and establish a good cost basis. Neutrino Factory R&D has reached a critical stage in which support is required for two key international experiments (MICE [126] and Targetry [127]) and a third-generation international design study. If this support is forthcoming, a Neutrino Factory could be added to the Neutrino Physics roadmap by the end of the decade.

Table 4: Considering a Neutrino Factory with simultaneous beams of positive and negative muons, the following 12 oscillation processes can in principle be studied.

$\mu^+ \to e^+\nu_e\overline{\nu}_\mu$	$\mu^- \to e^-\overline{\nu}_e$	
$\overline{\nu}_\mu \to \overline{\nu}_\mu$	$\nu_\mu \to \nu_\mu$	disappearance
$\overline{\nu}_\mu \to \overline{\nu}_e$	$\nu_\mu \to \nu_e$	appearance (challenging)
$\overline{\nu}_\mu \to \overline{\nu}_\tau$	$\nu_\mu \to \nu_\tau$	appearance (atm. oscillation)
$\nu_e \to \nu_e$	$\overline{\nu}_e \to \overline{\nu}_e$	disappearance
$\nu_e \to \nu_\mu$	$\overline{\nu}_e \to \overline{\nu}_\mu$	appearance: "golden" channel
$\nu_e \to \nu_\tau$	$\overline{\nu}_e \to \overline{\nu}_\tau$	appearance: "silver" channel

2.4.1 Oscillations physics at the Neutrino Factory

Of course the neutrinos coming from decays of muons of different charge must no be confused with each other, this can be done by timing provided the storage ring is adequately designed.

One of the most striking features of the Neutrino Factory is the precision with which the characteristics of all components of the beam should be known. This was studied extensively in the CERN yellow report [119], where the following were considered

- beam polarization effects, and its measurement with a polarimeter, allowing extraction of the beam energy, energy spread and verification that the polarization effects on the neutrino fluxes average out to zero with high precision;
- beam divergence effects, with the preliminary, conceptual study of a Cherenkov device to monitor the angular distribution of muons in the beam;
- radiative effects in muon decay;
- absolute normalization to be obtained both from a beam monitor, with the added possibility of an absolute cross-section normalization using the inverse muon decay reaction, $\nu_\mu e^- \to \mu^- \nu_e$, in the near detector.

with the conclusion that, in principle, a normalization of fluxes and cross-sections with a precision of 10^{-3} can be contemplated. Some of these features should also be present for a beta-beam, and for any facility in which a stored beam of well defined optical properties is used to produce neutrinos. This will be an essential difference with respect to the superbeams, where the knowledge of relative neutrino-vs-antineutrino cross-sections and fluxes will rely on the understanding of the initial particle production.
The Neutrino Factory lends itself naturally to the exploration of neutrino oscillations between ν flavors with high sensitivity. The detector should be able to perform both appearance and disappearance experiments, providing lepton identification and charge discrimination which is a tag for the initial flavor and of the oscillation. In particular the search for $\nu_e \to \nu_\mu$ transitions ("golden channel") appears to be very attractive at νF, because this transition can be studied in appearance mode looking for μ^- (appearance of wrong-sign μ) in neutrino beams where the neutrino type that is searched for is totally absent (μ^+ beam in νF).

The emphasis has been placed so far on small mixing angles and small mass differences. With two 40 Kt magnetic detectors (MINOS like) at 700 (or 7000) and 3000 km, with a

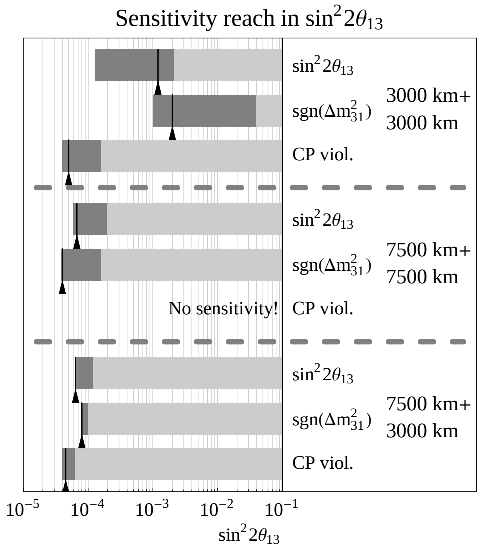

Figure 14: The sensitivity reaches of a 50 GeV Neutrino Factory as functions of $\sin^2 2\theta_{13}$ for $\sin^2 2\theta_{13}$ itself, the sign of $\Delta m^2_{31} > 0$, and (maximal) CP violation $\delta_{\rm CP} = \pi/2$ for each of the indicated baseline-combinations. The bars show the ranges in $\sin^2 2\theta_{13}$ where sensitivity to the corresponding quantity can be achieved at the 3σ confidence level. The dark bars mark the variations in the sensitivity limits by allowing the true value of Δm^2_{21} vary in the 3σ LMA-allowed range ($\Delta m^2_{21} \sim 4 \cdot 10^{-5}\,\mathrm{eV}^2 - 3 \cdot 10^{-4}\,\mathrm{eV}^2$). The arrows/lines correspond to the LMA best-fit value. Figure from [131].

conservative high energy muon detection threshold of 5 GeV, exposed to both polarity beams and 10^{21} muon decays, it will be possible to explore the θ_{13} angle down to $0.1°$ opening the possibility to measure the $\delta_{\rm CP}$ phase if $|\Delta m^2_{12}| \geq 5{\cdot}10^{-4}$ eV^2 [129, 79, 131].

On the other hand, the relative high energies of neutrinos selected by placing such a high threshold on muon energies require very long baselines for Neutrino Factories experiments (a 30 GeV neutrino has the first oscillation maximum at about 15000 km), and at these baselines CP asymmetries are dominated by matter effects [130]. Neutrino oscillation experiments with a high energy muon threshold, are then sensitive off the oscillation maximum (i.e. 3000 km for a 50 GeV Neutrino Factory) and such an experiment would be unable to unambiguously determine θ_{13} , $\delta_{\rm CP}$ and sign(Δm^2_{23}) .
Furthermore, as discussed in Section 1.3.2, the determination of ($\theta_{13}, \delta_{\rm CP}$) is not free of ambiguities and up to eight different regions of the parameter space can fit the same experimental result.
In order to solve these ambiguities, a single experimental point on a single neutrino beam is not enough.

One possibility is to envisage that all of β-beams, SuperBeams and Neutrino Factories will be available. Several investigations on how to solve this problem have been carried out, as reported in [113] and references therein. As an example the result of such an analysis combining the golden and the silver ($\nu_e \rightarrow \nu_\tau$) νF channels with the SPL-SB, taken from reference [120], is shown if Fig. 15.

A more interesting but challenging task will be to assume that only one of these facilities will become available (a more economical assumption!) and to investigate its ability to solve these ambiguities.

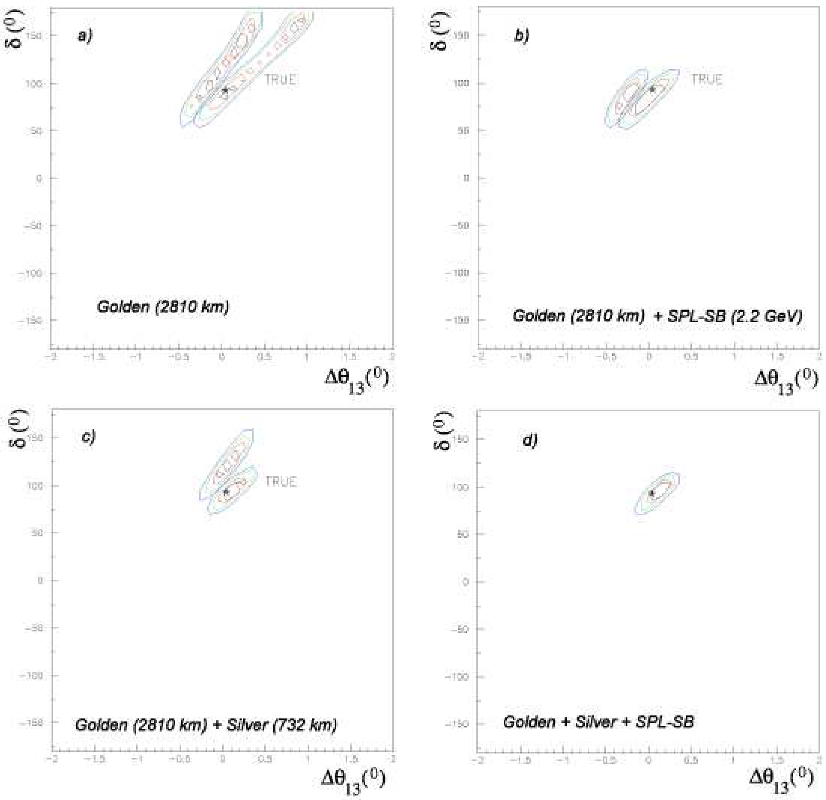

Figure 15: The results of a χ^2 fit for $\bar{\theta}_{13} = 2°; \bar{\delta}_{\rm CP} = 90°$. Four different combinations of experimental data are presented: a) magnetized iron detector (MID) at a νN; b) MID plus SPL-SB; c) MID plus hybrid emulsion (HE) at νF; d) the three detectors together. Notice how in case (d) the eightfold-degeneracy is solved and a good reconstruction of the physical $\theta_{13}, \delta_{\rm CP}$ values is achieved.

There are several handles to this problem at a Neutrino Factory. Clearly one should use more than just the wrong sign muons. Such a study was performed assuming the feasibility of a liquid argon detector [134]. By separating the events into several classes, right sign muon, wrong sign muon, electron and neutral current; and by performing a fine energy binning down to low energies; it was shown that i) the matter resonance could be neatly measured as shown in figure 16. The simultaneous observation of the four aforementioned channels was shown to allow resolution of ambiguities to a large extent.

The tau appearance channel *silver channel* [120] has been advocated as a powerful means of solving ambiguities. This can be readily understood since this channel has the opposite-sign dependence on δ_{CP} than the golden one, while having similar dependence on matter effects andθ_{13}. The principle of degeneracies-solving using several baselines, binning in energies and both silver and golden channels is explained on figure 17. The full demonstration that a neutrino factory alone with a complete set of appropriate detectors and two baselines could unambiguously do the job remains however to be demonstrated.

According to Tab. 4, Neutrino Factory potential could be further improved with a detector capable of measuring the charge of the electrons. R&D efforts for a liquid argon detector embedded in a magnetic fields are ongoing [133]; the first curved tracks were recently observed in a 10 liters Liquid Argon TPC embedded in magnetic field [135].

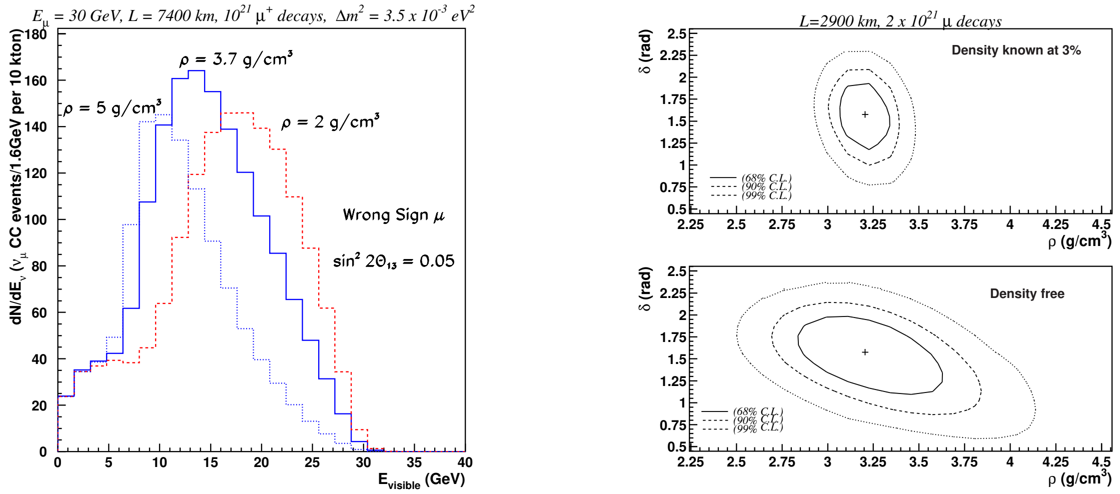

Figure 16: Left: variation of the MSW resonance peak for wrong sign muons as a function of Earths density. The plot is normalized to $10^{21}\mu^+$ decays. Right: result of a simultaneous fit to the matter density and to the CP phase for a 10kton detector situated 7000km away from a 30 GeV muon storage ring neutrino factory. Both plots from [134].

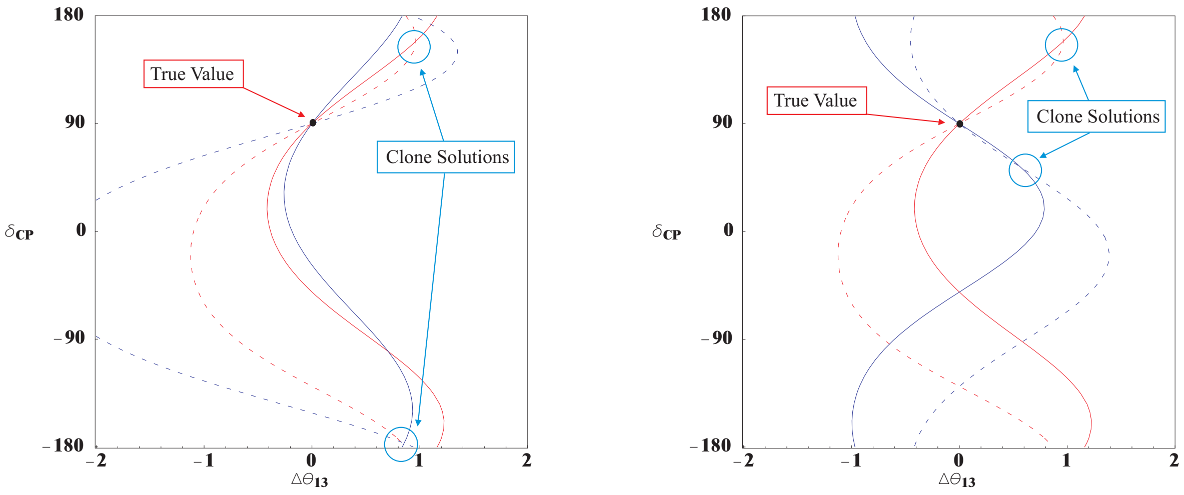

Figure 17: Solving the intrinsic degeneracy: two baseline L=730 and 3500 km, same channel example on the left, vs two channels $\nu_e \to \nu_\mu$ vs $\nu_e \to \nu_\tau$ same baseline example on the right.

3 Comparison

The comparison of performances of different facilities cannot be considered concluded. Several different aspects still need to be clarify before a final comparison can be performed.

- Costs, timescales, fluxes of the different accelerators systems are not yet fully computed.
- Performances of the detectors are not known at the same level: while for water Cerenkov detectors full simulation and full reconstructions of the events are available, based on the experience of SuperKamiokande (the only difference between SK and the megaton detector could be the photo detector coverage), the magnetic detector of neutrino factory performances are for the moment based on parametrization of the Minos performances. The emulsion detector for the silver channel of Nufact and the liquid argon detector are based on full simulations, not yet checked with the performances of the Opera and Icarus detectors respectively.
- Several different measurements can be defined as significative for the facility, and they cannot be optimized all together (see also reference [115]). For instance the following measurements bring to different optimizations: sensitivity to θ_{13} , discovery of subleading $\nu_\mu \to \nu_e$oscillations, unambiguous measurement of θ_{13} , measure of sign(Δm^2_{23}) , discovery of leptonic CP violation, unambiguous measurement of θ_{13} , sigdm and $\delta_{\rm CP}$.
- The final extraction of the oscillation parameters can significantly change based on technical aspects of the used programs (like choice of the input parameters, treatment of the errors on the other neutrino oscillation parameters, treatment of degeneracies etc.).

  From this point of view the introduction of the public domain, open source, Globes program [136] represents a major improvement: it allows to compare different facilities keeping the same the fitting program, and it makes explicit the description of the performances of the detectors. We strongly recommend that new developments in this field will make use of Globes, in view of a more transparent comparison of the different proposals.
- Systematic errors that strongly influence performances, for instance sensitivity to Leptonic CP violation for large values of θ_{13} , are not substantially discussed in the literature. We are confident that facilities where neutrino fluxes can be known a-priori, as the case of Beta Beams and Neutrino Factories, will have smaller systematic errors (and smaller backgrounds) of Neutrino SuperBeams. The quantity of this difference is not known at today
- Overall performances will depend by the combination of several different inputs. For instance low energy Super Beams and Beta Beams can profit of atmospheric neutrino oscillations, detected with a large statistics in the gigantic water Cerenkov detector, to solve degeneracies and measure sign(Δm^2_{23}) , as shown in the pioneering work of [114]. Neutrino factory can profit of the combination of different channels as the platinum, the golden and the silver one (see section 2.4), as well as detectors at different baselines. A full exploration of these possibilities is an ongoing process and the results available at today cannot be considered final

First we can quote the literature and show some comparison.

Then I would propose to take what is available in the Globes library and make a comparison by ourselves. I can do it in a couple of days and we can ask Patrick to redo the same thing.

References

[1] C. Weinheimer, Nucl. Phys. Proc. Suppl. **118** (2003) 279.

[2] V. M. Lobashev *et al.*, Nucl. Phys. Proc. Suppl. **91** (2001) 280. V. M. Lobashev, proceeding of "Neutrino Telescopes 2005", Venice, pg. 507-517

[3] KATRIN Coll., hep-ex/0109033.

[4] A. Monfardini *et al.*, arXiv:hep-ex/0509038.

[5] K.A. Assamagan *et al.*, Phys. Rev. **D53**, 6065 (1996).

[6] R. Barate *et al.*, Eur. Phys. J. **C1**, 395 (1998).

[7] W.H. Furry, Phys. Rev. **56**, 1184 (1939); for reviews, see M. Doi, T. Kotani and E. Takasugi, Prog. of Theor. Phys. Suppl. **83**,1 (1985); H.V. Klapdor-Kleingrothaus, World Scientific, Singapore (2001).

[8] E. Majorana, Nuovo Cimento **14**, 171 (1937).

[9] H. V. Klapdor-Kleingrothaus, A. Dietz and I. V. Krivosheina, Found. Phys. **32** (2002) 1181 [Erratum-ibid. **33** (2003) 679] [arXiv:hep-ph/0302248].

[10] Y. G. Zdesenko, F. A. Danevich and V. I. Tretyak, Phys. Lett. B **546** (2002) 206.

[11] A. M. Bakalyarov, A. Y. Balysh, S. T. Belyaev, V. I. Lebedev and S. V. Zhukov [C03-06-23.1 Collaboration], Phys. Part. Nucl. Lett. **2** (2005) 77 [Pisma Fiz. Elem. Chast. Atom. Yadra **2** (2005) 21] [arXiv:hep-ex/0309016].

[12] C. Arnaboldi *et al.*, Phys. Rev. Lett. **95** (2005) 142501 [arXiv:hep-ex/0501034].

[13] R. Arnold *et al.* [NEMO Collaboration], arXiv:hep-ex/0507083.

[14] R. Ardito *et al.*, arXiv:hep-ex/0501010.

[15] S. Schonert *et al.* [GERDA Collaboration], Nucl. Phys. Proc. Suppl. **145** (2005) 242.

[16] C. L. Bennett et al., Astrophys. J. Suppl. 148, 1 (2003).

[17] D. G. York et al., Astron. J. 120, 159 (2000).

[18] M. Fukugita and T. Yanagida, Phys. Lett. B174, 45 (1986).

[19] W. Buchmüller, P. Di Bari and M. Plümacher, Nucl. Phys. B665, 445 (2003).

[20] G. F. Giudice, A. Notari, A. Riotto and A. Strumia, Nucl. Phys. B685, 89 (2004).

[21] W. Buchmüller, P. Di Bari and M. Plümacher, Ann. Phys. 315, 303 (2005).

[22] D.N. Spergel et al., Astrophys. J. Suppl. 148, 175 (2003).

[23] M. Tegmark et al., Phys. Rev. D69, 103501 (2004).

[24] D. Eisenstein et al., arXiv:astro-ph/0501171

[25] M. Tegmark et al., Astrophys. J. 606, 702 (2004).

[26] S. Cole et al., Mon. Not. Roy. astr. Soc. 362, 505 (2005).

[27] W. Hu, D. J. Eisenstein and M. Tegmark, Phys. Rev. Lett. 80, 5255 (1998).

[28] R. Valdarnini, T. Kahniashvili and B. Novosyadlyj, Astron. Astrophys. 336, 11 (1998).

[29] S. Hannestad, JCAP 5. 004 (2003).

[30] S.W. Allen, R.W. Schmidt and S.L. Bridle, Mon. Not. Roy. astr. Soc. 346, 593 (2003).

[31] V. Barger, D. Marfatia and A. Tregre, Phys. Lett. B595, 55 (2004).

[32] R.A.C. Croft, D.H. Weinberg, N. Katz and L. Hernquist, Astrophys. J. 495, 44 (1998).

[33] P. McDonald et al., arXiv:astro-ph/0405013

[34] U. Seljak et al., arXiv:astro-ph/0407372

[35] R.A.C. Croft, W. Hu and R. Davé, Phys. Rev. Lett. 83, 1092 (1999).

[36] Ø. Elgarøy and O. Lahav, New J. Phys. 7, 61 (2005).

[37] Precision Electroweak Measurements on the Z Resonance The LEP collaborations, hep-ex/0509008, to appear as physics report.

[38] B. T. Cleveland *et al.*, Astrophys. J. **496** (1998) 505.

[39] M. Altmann *et al.* [GNO Collaboration], Phys. Lett. B **490** (2000) 16 [arXiv:hep-ex/0006034].

[40] J. N. Abdurashitov *et al.* [SAGE Collaboration], J. Exp. Theor. Phys. **95** (2002) 181 [Zh. Eksp. Teor. Fiz. **122** (2002) 211] [arXiv:astro-ph/0204245].

[41] S. Fukuda *et al.* [Super-Kamiokande Collaboration], Phys. Lett. B **539** (2002) 179 [arXiv:hep-ex/0205075].

[42] S. N. Ahmed *et al.* [SNO Collaboration], Phys. Rev. Lett. **92** (2004) 181301 [arXiv:nucl-ex/0309004].

[43] K. Eguchi *et al.* [KamLAND Collaboration], Phys. Rev. Lett. **90** (2003) 021802 [arXiv:hep-ex/0212021]. T. Araki *et al.* [KamLAND Collaboration], Phys. Rev. Lett. **94** (2005) 081801 [arXiv:hep-ex/0406035].

[44] Y. Fukuda *et al.* [Super-Kamiokande Collaboration], Phys. Rev. Lett. **81** (1998) 1562 [arXiv:hep-ex/9807003].

[45] M. C. Sanchez *et al.* [Soudan 2 Collaboration], Phys. Rev. D **68** (2003) 113004 [arXiv:hep-ex/0307069].

[46] M. Ambrosio *et al.* [MACRO Collaboration], Phys. Lett. B **566** (2003) 35 [arXiv:hep-ex/0304037].

[47] Y. Ashie *et al.* [Super-Kamiokande Collaboration], Phys. Rev. Lett. **93** (2004) 101801 [arXiv:hep-ex/0404034].

[48] M. Apollonio *et al.* [CHOOZ Collaboration], Eur. Phys. J. C **27** (2003) 331, [arXiv:hep-ex/0301017].

[49] A. Guglielmi, M. Mezzetto, P. Migliozzi and F. Terranova, arXiv:hep-ph/0508034.

[50] E. Aliu *et al.* [K2K Collaboration], Phys. Rev. Lett. **94** (2005) 081802 [arXiv:hep-ex/0411038].

[51] L. Wolfenstein, Phys. Rev. D17 (1978) 2369. S.P. Mikheev and A.Y. Smirnov, Nuovo Cim. C9 (1986) 17.

[52] K. Kimura, A. Takamura and H. Yokomakura, Phys. Rev. D **66** (2002) 073005 [arXiv:hep-ph/0205295]. E. K. Akhmedov, R. Johansson, M. Lindner, T. Ohlsson and T. Schwetz, JHEP **0404** (2004) 078 [arXiv:hep-ph/0402175]. M. Freund, Phys. Rev. D **64** (2001) 053003 [arXiv:hep-ph/0103300].

[53] G. L. Fogli, E. Lisi, A. Marrone and A. Palazzo, arXiv:hep-ph/0506083.

[54] A. Aguilar *et al.* [LSND Collaboration], Phys. Rev. D **64** (2001) 112007 [arXiv:hep-ex/0104049].

[55] B. Armbruster *et al.* [KARMEN Collaboration], Phys. Rev. D **65** (2002) 112001 [arXiv:hep-ex/0203021].

[56] P. Astier *et al.* [NOMAD Collaboration], Phys. Lett. B **570** (2003) 19 [arXiv:hep-ex/0306037].

[57] E. Church *et al.* [BooNe Collaboration], arXiv:nucl-ex/9706011.

[58] E. Ables *et al.* [MINOS Collaboration], Fermilab-proposal-0875 G. S. Tzanakos [MINOS Collaboration], AIP Conf. Proc. **721**, 179 (2004).

[59] The Fermilab NuMI Group, "NumI Facility Technical Design Report", Fermilab Report NuMI-346, 1998.

[60] F. Arneodo *et al.* [ICARUS Collaboration], Nucl. Instrum. and Meth. A **461** (2001) 324; P. Aprili *et al.*, "The ICARUS experiment", CERN-SPSC/2002-27, SPSC-P-323.

[61] OPERA Collaboration, CERN-SPSC-P-318, LNGS-P25-00; H. Pessard [OPERA Collaboration], arXiv:hep-ex/0504033.M. Guler *et al.* [OPERA Collaboration], "OPERA: An appearance experiment to search for $\nu_\mu \to \nu_\tau$ oscillations in the CNGS beam. Experimental proposal," CERN-SPSC-2000-028.

[62] G. Acquistapace *et al.*, "The CERN neutrino beam to Gran Sasso", CERN 98-02, INFN/AE-98/05 (1998); CERN-SL/99-034(DI), INFN/AE-99/05 Addendum.

[63] H. W. Atherton *et al.*, "Precise measurements of particle production by 400 GeV/c protons on Beryllium targets," CERN-80-07.

[64] G. Ambrosini *et al.* [NA56/SPY Collaboration], Eur. Phys. J. C **10** (1999) 605.

[65] L. Casagrande *et al.*, “The alignment of the CERN West Area neutrino facility,” CERN-96-06.

[66] A. Guglielmi and G. Collazuol, “Monte Carlo Simulation of the SPS WANF Neutrino Flux”, INFN/AE-03/05 (2003).
P. Astier *et al.* [NOMAD Collaboration], Nucl. Instrum. Meth. A **515** (2003) 800 [arXiv:hep-ex/0306022].

[67] A. Ferrari, A. Guglielmi and P. R. Sala, Nucl. Phys. Proc. Suppl. **145** (2005) 93 [arXiv:hep-ph/0501283].

[68] Report to the Fermilab Director by the Proton Committee, November 9, 2004, `http://www.fnal.gov/directorate/program_planning/Nov2004PACPublic/Draft_Proton_Plan_v2.pdf`

[69] M. Komatsu, P. Migliozzi and F. Terranova, J. Phys. G **29** (2003) 443 [arXiv:hep-ph/0210043].

[70] P. Migliozzi and F. Terranova, Phys. Lett. B **563** (2003) 73 [arXiv:hep-ph/0302274].

[71] M. Benedikt, K. Cornelis, R. Garoby, E. Metral, F. Ruggiero and M. Vretenar, “Report of the High Intensity Protons Working Group,” CERN-AB-2004-022-OP-RF.

[72] F. Ardellier *et al.* [Double-CHOOZ Collaboration], arXiv:hep-ex/0405032.

[73] A. De Rujula, M.B. Gavela, P. Hernandez, Nucl. Phys. B547 (1999) 21, arXiv: hep-ph/9811390.

[74] Q. R. Ahmad et al., SNO Coll., nucl-ex/0204008.

[75] 'ECFA/CERN studies of a European Neutrino Factory complex', A. Blondel et al, ed CERN 2004-002 (2004) http://preprints.cern.ch/cernrep/2004/2004-002/2004-002.html

[76] Beams for European Neutrino Experiments is a Neworking Activity (http://bene.na.infn.it/) supported by the EC and most major European Agencies in the framework of the FP6 Integrated Activity CARE (Coordinated Accelerator R&D in Europe) http://esgard.lal.in2p3.fr/Project/Activities/Current/. The scope of BENE is also described in more detail in the following document: http://esgard.lal.in2p3.fr/Project/Activities/Current/Networking/N3/BENE-downsized-11.doc

[77] Workshop on Physics at a Multi Megawatt Proton driver, CERN-SPSC-2004-SPSC-M-722,

[78] B. Richter, SLAC-PUB-8587 [arXiv:hep-ph/0008222], and references therein.

[79] J. Burguet-Castell, M. B. Gavela, J. J. Gomez-Cadenas, P. Hernandez and O. Mena, Nucl. Phys. B **608** (2001) 301 [arXiv:hep-ph/0103258].

[80] H. Minakata and H. Nunokawa, JHEP **0110** (2001) 001 [arXiv:hep-ph/0108085].

[81] V. Barger, D. Marfatia and K. Whisnant, Phys. Rev. D **65** (2002) 073023 [arXiv:hep-ph/0112119].

[82] G. L. Fogli and E. Lisi, Phys. Rev. D **54** (1996) 3667 [arXiv:hep-ph/9604415].

[83] M.G. Catanesi *et al.* [HARP Collaboration], CERN-SPSC/2001-017, SPSC/P322, May 2001.

[84] S. Geer, Phys. Rev. D **57** (1998) 6989 [Erratum-ibid. D **59** (1999) 039903], [hep-ph/9712290].

[85] P. Zucchelli, Phys. Lett. B **532** (2002) 166.

[86] 'Feasibility Study-II of a Muon-Based Neutrino Source', S. Ozaki, R. Palmer, M. Zisman, and J. Gallardo, eds. BNL-52623, June 2001, available at http://www.cap.bnl.gov/mumu/studyii/FS2-report.html ; M.M. Alsharo'a et al., Phys. Rev. ST Accel. Bemas 6, 081001 (2003).

[87] Y. Itow *et al.*, "The JHF-Kamiokande neutrino project", arXiv:hep-ex/0106019.

[88] The E889 Collaboration, "Long Baseline Neutrino Oscillation Experiment at the AGS", Brookhaven National Laboratory Report BNL No. 52459, April 1995. A. Para and M. Szleper, arXiv:hep-ex/0110032.

[89] D. S. Ayres *et al.* [NOvA Collaboration], arXiv:hep-ex/0503053.

[90] M. V. Diwan *et al.*, Phys. Rev. D **68** (2003) 012002 [arXiv:hep-ph/0303081].

[91] B. Autin *et al.*, CERN-2000-012

[92] J. J. Gomez-Cadenas *et al.*, hep-ph/0105297.
A. Blondel *et al.*, Nucl. Instrum. Meth. A **503** (2001) 173. M. Mezzetto, J.Phys.G29:1771-1776, 2003; hep-ex/0302005.

[93] J. J. Gomez-Cadenas *et al.*, Proceedings of "Venice 2001, Neutrino telescopes", vol. 2*, 463-481, arXiv:hep-ph/0105297. A. Blondel *et al.*, Nucl. Instrum. Meth. A **503** (2001) 173. M. Mezzetto, J. Phys. G **29** (2003) 1771 [arXiv:hep-ex/0302005].

[94] L. Mosca, Nucl. Phys. Proc. Suppl. **138** (2005) 203.

[95] M. Apollonio *et al.*, arXiv:hep-ph/0210192.

[96] J. E. Campagne and A. Cazes, arXiv:hep-ex/0411062.

[97] R. Garoby, "The SPL at CERN," CERN-AB-2005-007.

[98] C. K. Jung [UNO Collaboration] arXiv:hep-ex/0005046.

[99] `http://www.ganil.fr/eurisol/`

[100] J. Nolen, NPA 701 (2002) 312c

[101] P. Sortais, presentations at the Moriond workshop on radioactive beams, Les Arcs (France) 2003 "ECR technology", `http://moriond.in2p3.fr/radio`

[102] M. Benedikt, S. Hancock and J-L. Vallet, CERN note AB-Note-2003-080 MD

[103] M. Mezzetto, Nucl. Phys. Proc. Suppl. **149** (2005) 179.

[104] M. Mezzetto, arXiv:hep-ex/0511005.

[105] B. Autin *et al.*, arXiv:physics/0306106. M. Benedikt, S. Hancock and M. Lindroos, Proceedings of EPAC 2004, http://accelconf.web.cern.ch/AccelConf/e04.

[106] M. Mezzetto, J.Phys. G **29** (2003) 1781 [arXiv:hep-ex/0302007]. J. Bouchez, M. Lindroos and M. Mezzetto, AIP conference proceedings, **721** (2003) 37 [arXiv:hep-ex/0310059]. M. Mezzetto, Nucl. Phys. Proc. Suppl. **143** (2005) 309 [arXiv:hep-ex/0410083].

[107] A. Donini, E. Fernandez-Martinez, P. Migliozzi, S. Rigolin and L. Scotto Lavina, Nucl. Phys. B **710** (2005) 402 [arXiv:hep-ph/0406132].

[108] M. Lindroos, EURISOL DS/TASK12/TN-05-02.

[109] J. Burguet-Castell, D. Casper, E. Couce, J. J. Gomez-Cadenas and P. Hernandez, arXiv:hep-ph/0503021.

[110] J. Burguet-Castell *et al.*, Nucl. Phys. B **695** (2004) 217 [arXiv:hep-ph/0312068].

[111] F. Terranova, A. Marotta, P. Migliozzi and M. Spinetti, Eur. Phys. J. C **38** (2004) 69 [arXiv:hep-ph/0405081].

[112] O. Bruning *et al.*, "LHC luminosity and energy upgrade: A feasibility study," CERN-LHC-PROJECT-REPORT-626.

[113] A. Donini, AIP Conf. Proc. **721** (2004) 219 [arXiv:hep-ph/0310014].

[114] P. Huber, M. Maltoni and T. Schwetz, Phys. Rev. D **71** (2005) 053006 [arXiv:hep-ph/0501037].

[115] P. Huber et al., arXiv:hep-ph/0506237.

[116] A. Donini, E. Fernandez, P. Migliozzi, S. Rigolin, T. T. de Fatis and F. Terranova, arXiv:hep-ph/0511134.

[117] J. Bernabeu, J. Burguet-Castell, C. Espinoza and M. Lindroos, hep-ph/0505054

[118] J. Sato, hep-ph/0503144.

[119] A. Blondel et al eds., *ECFA/CERN studies of a European Neutrino Factory complex*, CERN 2004-002 (2004) http://preprints.cern.ch/cernrep/2004/2004-002/2004-002.html

[120] A. Donini, D. Meloni, P. Migliozzi, Nucl. Phys. B646 (2002) 321, hep-ph/0206034; D. Autiero *et al.*, Eur. Phys. J. C **33** (2004) 243 [arXiv:hep-ph/0305185]. S. Rigolin, Rencontres de Moriond 2004, hep-ph/0407009.

[121] S. Geer, Phys. Rev. D57 (1998) 6989; A. De Rjula, M.B. Gavela and P. Hernndez, Nucl. Phys. B547 (1999) 21; A. Blondel et al., Nucl. Instrum. Methods Phys. Res., A 451 (2000) 102; For recent reviews see M. Apollonio, et al, in CERN-04/02, (2004) arXiv:hep-ex/0210192; J. J. Gmez-Cadenas and D.A. Harris, "Physics opportunities at neutrino factories," Ann. Rev. Nucl. Part. Sci. 52 (2002) 253 and the annual proceedings of the International Nufact Workshop.

[122] B. Autin, A. Blondel and J. Ellis eds, CERN yellow report CERN 99-02, ECFA 99-197

[123] P. Gruber et al, 'The Study of a European Neutrino Factory Complex', Neutrino Factory Note 103(2002) CERN/PS/2002-080(PP) , in 'ECFA/CERN Studies of a European Neutrino Factory Complex ' Blondel, A (ed.) et al.CERN-2004 002.- ECFA-04-230, p7

[124] The Muon Collider and Neutrino Factory Collaboration, see the web site http://www.cap.bnl.gov/mumu/ which contains also references to several physics studies.

[125] Feasibility Study on a Neutrino Source Based on a Muon Storage Ring, D.Finley, N.Holtkamp, eds. (2000), http://www.fnal.gov/projects/muon_collider/reports.html

[126] The International Muon Ionization Experiment MICE, http://hep04.phys.iit.edu/cooldemo

[127] R.J. Bennett et al, 'Studies of a target system for a 4MW 24 GeV proton beam', CERN-INTC proposal 2003-033, April 2004.

[128] "Neutrino Factory and Beta Beam Experiments and Developments", (Eds. S. Geer and M. Zisman), Report of the Neutrino Factory and Beta Beam Working Group, APS Multi-Divisional Study of the Physics of Neutrinos, July 2004.

[129] A. Cervera, F. Dydak and J. Gomez Cadenas, Nucl. Instrum. Meth. A **451** (2000) 123.

[130] S. Geer, Comments Nucl. Part. Phys. A **2** (2002) 284 [arXiv:hep-ph/0008155].

[131] P. Huber and W. Winter; Phys. Rev. D68, 037301(2003); hep/ph-0301257.

[132] A Feasibility Study of A Neutrino Factory in Japan, Y. Kuno, ed., http://www-prism.kek.jp/nufactj/index.html

[133] A. Ereditato and A. Rubbia, arXiv:hep-ph/0510131.

[134] A. Bueno, M. Campanelli, A. Rubbia, Nucl. Phys. B **589** (2000) 577 [arXiv:hep-ph/0005007].

[135] A. Badertscher et al, physics/0505151.

[136] P. Huber, M. Lindner and W. Winter, Comput. Phys. Commun. **167** (2005) 195 [arXiv:hep-ph/0407333].